



TECHNISCHE  
UNIVERSITÄT  
WIEN  
Vienna University of Technology

## Diplomarbeit

# Development of a standard addition method for quantitative LA-ICP-MS analysis

Ausgeführt am Institut für Chemische Technologien und Analytik  
der Technischen Universität Wien

unter der Anleitung von

**Univ.Prof. Dipl.-Ing. Dr.techn. Limbeck Andreas**

durch

**Konrad Bielecki BSc**

Die approbierte gedruckte Originalversion dieser Diplomarbeit ist an der TU Wien Bibliothek verfügbar  
The approved original version of this thesis is available in print at TU Wien Bibliothek.

## Abstract

Liquid Inductively coupled plasma mass spectrometry (=ICP-MS) offers an established method for the quantification of trace elements in various samples. However, the need to digest solid samples first risks contamination and creates a high workload. This approach also only offers bulk information. Circumventing this with LA-ICP-MS measurements is preferable but it also has its problems. The difficulty hereby lies in the quantification process. Certified reference materials are expensive, not available for novel materials, and often do not match the matrix of the sample material precisely. This creates a massive problem when researching new materials of unknown composition and forces one to develop workaround in house methods like the dry droplet technique, microwells or preparation of powdered pellets or tablets. However, those are often hamstrung by issues of inhomogeneity and replicability.

This research is dedicated to developing a new standard addition method to circumvent those problems and make it applicable to polymer films. An HTX TM-Sprayer was used to evenly deposit liquid standards onto the surface of polymer films. This process was optimized with a series of experiments varying the composition of the solvent by changing the concentration of Polyethylene glycol (PEG), Isopropanol, and water, to achieve a homogeneous distribution of residues after solvent evaporation. Variation of dissolved analyte allows preparation of standards with known contents, which were then measured with LA-ICP-MS, resulting in a calibration function. Measurements of identical standards show a standard deviation of 0.68 %. The standards can further be created and stored for multiple months without any changes to their quality, indicating very good stability at 20 to 25 °C.

Liquid ICP-MS measurements of those sprayed and microwave digested standards were performed to determine the relation of the elemental concentrations in the applied liquid standards to the respective amounts in the applied coating, which resulted in a factor dependent on the thickness and density of the investigated material. This factor was then used to modify the previously obtained calibration curve. The developed method was then applied to determine the concentration of native Sulfur in a commercially acquired Kapton film.

The results were evaluated with a reference measurement since there were no Certified Reference Materials available at the time of this work. Microwave assisted acid digestions of unsprayed Kapton were performed and the solutions were analyzed with liquid ICP-MS. The results derived with both methods are in good accordance.

Additional polymer films, namely Nafion® and Polystyrene film, were also investigated and evaluated. The obtained results show good properties in terms of linearity, applicability, and reproducibility on

other polymers. This new standard addition method further shows great potential for flexible calibration of a wide array of elements such as S, Pb, Zn, Sn, Ag, etc. Additional experiments also show promising results for other substrates like Cu, Si, or Al.

However, it was not possible to successfully execute reference measurements for all samples due to stability issues of certain polymers such as Nafion® and the inability to perform liquid ICP-MS.

## Kurzfassung

Liquid Inductively coupled plasma mass spectrometry (=ICP-MS) bietet eine etablierte Methode zur Quantifizierung von Spurenelementen in verschiedenen Proben. Die Notwendigkeit feste Proben zuerst aufzuschließen, birgt jedoch das Risiko einer Kontamination und verursacht einen hohen Arbeitsaufwand. Weiters bietet dieser Ansatz nur Information über den Bulk der untersuchten Probe. Dies mit LA-ICP-MS-Messungen zu umgehen ist vorzuziehen, hat aber auch seine Probleme. Die Schwierigkeit hierbei liegt im Quantifizieren der erhaltenen Messdaten. Zertifizierte Referenzmaterialien sind teuer, oft nicht verfügbar für neuartige Materialien und oft passen sie auch nicht genau zur Matrix des Probenmaterials. Diese Probleme sind ein massives Hindernis bei der Erforschung neuer Materialien unbekannter Zusammensetzung und zwingt dazu, in-house Methoden zur Problemquantifizierung zu entwickeln. Beispiele hierzu sind die dried droplet Technik, Mikrovertiefungen oder die Herstellung von pulverförmigen, gepressten Pellets oder Tabletten. Jedoch werden diese oft durch Inhomogenität und Reproduzierbarkeit gelähmt.

Diese Arbeit widmet sich der Entwicklung einer neuen Standardadditionsmethode, um diese Probleme zu umgehen und sie auf Polymerfolien anwendbar zu machen. Ein HTX TM-Sprayer wurde verwendet, um flüssige Standards gleichmäßig auf die Oberfläche von Polymerfilmen aufzutragen. Dieser Prozess wurde durch eine Reihe von Experimenten optimiert, bei denen die Zusammensetzung des Lösungsmittels durch Änderung der Konzentration von Polyethylenglykol (PEG), Isopropanol und Wasser variiert wurde, um eine homogene Verteilung der Rückstände nach der Lösungsmittelverdampfung zu erreichen. Die Variation des gelösten Analyten ermöglicht die Herstellung von Standards mit bekannten Inhalten, die dann mit LA-ICP-MS gemessen wurden, was zu einer Kalibrierungsfunktion führte. Messungen identischer Standards zeigten eine Standardabweichung von 0,68 %. Darüber hinaus können die hergestellten Standards ohne Qualitätsveränderungen über mehrere Monate gelagert werden, was eine sehr gute Stabilität bei 20 bis 25 °C nahelegt.

Flüssig-ICP-MS-Messungen dieser gesprühten und mikrowellenaufgeschlossenen Standards wurden durchgeführt, um das Verhältnis der Elementkonzentrationen in den aufgetragenen flüssigen Standards zu den jeweiligen Mengen in der aufgetragenen Beschichtung zu bestimmen, wobei dies zu einem Faktor führte, welcher von der Dicke und Dichte des untersuchten Probenmaterials abhängig ist. Dieser Faktor wurde dann verwendet, um die zuvor erhaltene Kalibrierungskurve zu modifizieren. Die entwickelte Methode wurde dann angewendet, um die Konzentration von nativem Schwefel in einer kommerziell erworbenen Kapton® Folie zu bestimmen.

Die Ergebnisse wurden mit einer Referenzmessung ausgewertet, da zum Zeitpunkt dieser Arbeit noch keine zertifizierten Referenzmaterialien der untersuchten Proben zur Verfügung standen. Es wurden

mikrowellenunterstützte Säureaufschlüsse von unbesprühtem Kapton durchgeführt und die Lösungen mit flüssigem ICP-MS analysiert. Die mit beiden Verfahren erzielten Ergebnisse stimmen gut überein.

Auch weitere Polymerfolien, nämlich Nafion® und Polystyrolfolie, wurden untersucht und bewertet. Die erhaltenen Ergebnisse zeigen gute Eigenschaften hinsichtlich Linearität, Anwendbarkeit und Reproduzierbarkeit auf andere Polymere. Diese neue Standardadditionsmethode zeigt außerdem großes Potenzial für die flexible Kalibrierung einer breiten Palette von Elementen wie S, Pb, Zn, Sn, Ag usw. Zusätzliche Experimente zeigen auch vielversprechende Ergebnisse für andere Substrate wie Cu, Si oder Al.

Aufgrund von Stabilitätsproblemen bei bestimmten Polymeren wie Nafion® und der Unfähigkeit, Flüssig-ICP-MS durchzuführen, war es jedoch nicht möglich Referenzmessungen für alle Proben erfolgreich durchzuführen.

# Contents

Abstract .....	2
Kurzfassung .....	4
1. Introduction.....	8
2. Theoretical Aspects .....	10
2.1 ICP-MS.....	10
2.1.1 Overview .....	10
2.1.2 Laser.....	13
2.1.3 ICP .....	14
2.1.4 MS.....	15
2.2 Quantification Methods for LA-ICP-MS.....	16
2.2.1 Certified Reference Materials (CRM).....	16
2.2.2 In-house made standards for quantitative analysis .....	17
3. Experimental .....	20
3.1 Instrumental.....	20
3.2 Method scheme .....	23
3.3 Standard preparation.....	24
3.4 Polymer Film Substrate Preparation.....	27
3.5 LA-ICP-MS measurement .....	29
3.6 Microwave-assisted acid digestion and liquid ICP-MS analysis .....	31
4. Results and Discussion .....	34
4.1 Initial Experiments .....	34
4.2 Area specific mass deposition of the standard .....	39
4.3 Determination of concentration in the polymer film .....	41
4.4 Validation .....	43
4.5 Results polymer film .....	45
4.6 Other Polymer Substrates.....	48
4.7 Non-Polymer Substrates .....	53

5. Conclusion .....	62
6. Literature / References.....	64
7. Appendix.....	68

# 1. Introduction

Laser ablation inductively coupled plasma mass spectrometry (LA-ICP-MS) is an analytical technology that utilizes a high-power laser pulse to ablate a well-defined area of a target material. This process generates fine particles in form of an aerosol which is subsequently transported to a plasma that functions as a secondary ionization source. The atomized and ionized elements are further transported into a mass spectrometer to determine the elemental and isotopic composition of the investigated material [1]. This technology allows for a wide application range and is used in environmental chemistry [2], geochemistry [3], life science [4], material science [5], and many more.

LA-ICP-MS combines the low detection limits with high spatial resolution to provide accurate and precise data about the elemental content in a specific sample. However, the acquisition of quantitative information requires the application of matrix matched standards or certified reference materials with identical elemental composition [6]. This is due to the matrix effect during the ablation process, which leads to vastly different amounts of material being transported to the ICP-MS. It also influences the atomization and excitation efficiency of the method [7]. Certified reference materials are however very rare and costly, especially for novel materials in the rapidly changing and developing landscape of polymers.

To overcome this problem, work intensive preparations and characterization of in-house standards need to be conducted to lessen the impact of matrix effects. Usually for this purpose a digestion or the grinding of solid material is necessary, followed by an analysis of the derived sample solution or the creation of pellets and tablets to be analysed. This can however be challenging for inert materials such as polymers, which are also difficult to grind.

To minimize the time intensive and laborious calibration process an alternative is needed. Approaches using liquid standard solutions exist, which allow for a flexible preparation of various concentration levels for several elements. Two application concepts are reported in literature so far, dried droplets [32] and  $\mu$ -wells or grooves [31]. However, microwells and grooves are difficult to apply because the volume staying behind in those wells is not known and needs to be investigated through other, difficult to execute means. The need to dissolve or suspend the target material also makes the analysis a laborious process with some specimen not being fit for study altogether. Dried droplet evaporation is currently the best way to circumvent this and sees widespread use, especially in applications surrounding mass spectrometry. But this method comes with a plethora of issues like the coffee ring effect and reproducibility problems due to the “Hot Spots” phenomenon.

This warrants the development of a new quantification approach for polymer films via LA-ICP-MS with the possibility of an application on other solid samples, like metals, glass, silicon, or ceramics. The new



alternative is the application of a standard addition technique to apply a layer of a well-defined substance to the surface of the sample to ablate it and create a linear calibration in the process. One such procedure for reproducible deposition of a small coating layer utilizes inkjet printing and was developed by Bonet et al. [44]. The problem hereby is the limited solubility of metal standards in ink. The idea to overcome this limitation is to adapt the approach used in MALDI for deposition of the matrix on the sample surface.

However, this requires the additional use of another machine, an HTX-sprayer, to apply the standard layer. The standard addition solutions for the calibration are prepared beforehand with various analyte concentrations in a carrier solution that vaporizes during the spray process, leaving behind a solid, homogeneously distributed coating of a matrix and the desired elements.

The goal of this work is to develop and optimize the afore mentioned standard addition method for commercially available polymer films to create reliable and reproducible results for a multitude of elements. Of special interest is Sulfur due to its abundance in the investigated polymer film Kapton®.

The developed standard calibration approach was then applied to a variety of materials (Aluminum, Copper, glass, LTCC, Silicon-wafer, Silicon carbide) to determine its applicability to other materials.

## 2. Theoretical Aspects

### 2.1 ICP-MS

#### 2.1.1 Overview

Inductively coupled plasma mass spectrometry (ICP-MS) offers us two approaches to quantitative analysis of solid samples. The first being the direct analysis of the solid sample using laser ablation ICP-MS (LA-ICP-MS) or the conversion of the solid material into a solution with subsequent liquid ICP-MS of the prepared sample solution.

An overview can be seen in Figure 1.

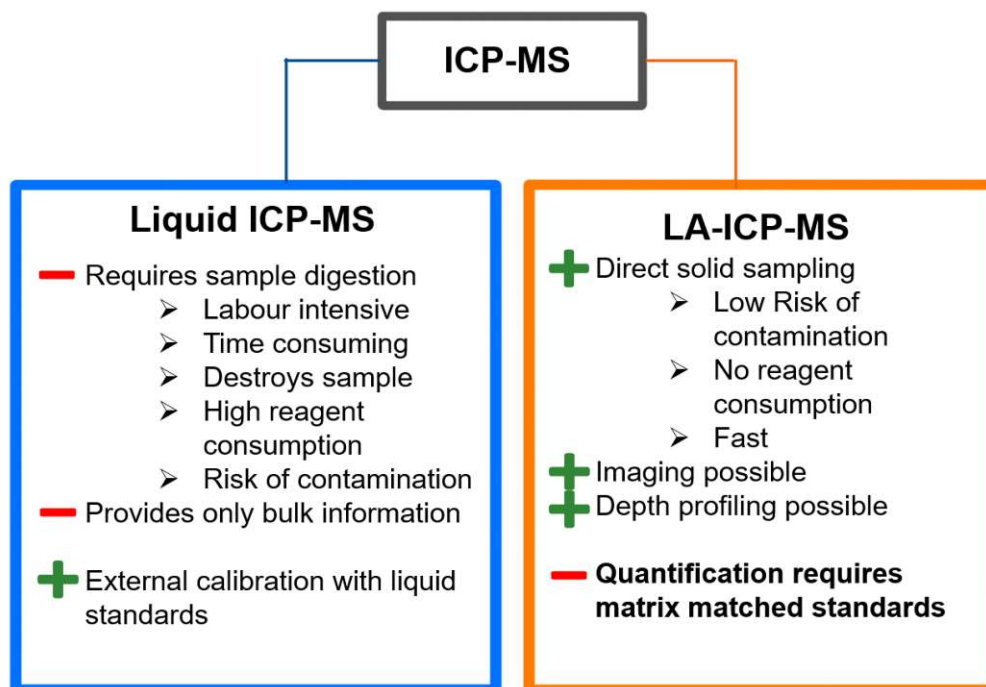


Figure 1 Pros and cons overview liquid ICP-MS and LA-ICP-MS [2][13][15]

The laser ablation inductively coupled plasma mass spectrometry (LA-ICP-MS) system offers us the ability to directly measure solid samples, which lowers the risk of contamination, consumes no reagents, offers us fast information about the sample composition, has limited sample consumption, and is a spatially resolved analysis method. Although possible sample imaging as well as the creation of depth profiles was not utilized in this work.

The LA-ICP-MS system can be divided into three parts, which can be seen in Figure 2.

- The first part consists of a laser system capable of vaporizing solid samples. A camera/microscope is used to find the desired ablation spot by moving the ablation cell with an X-Y-Z stage.
- The ablated material aerosol is transported to the ICP with a steady gas flow of argon or helium. The particles are introduced into the plasma where they are atomized and ionized.
- The generated ions are then transferred into a mass spectrometer for detection. This results in qualitative and quantitative information about the sample's elemental and isotopic composition.

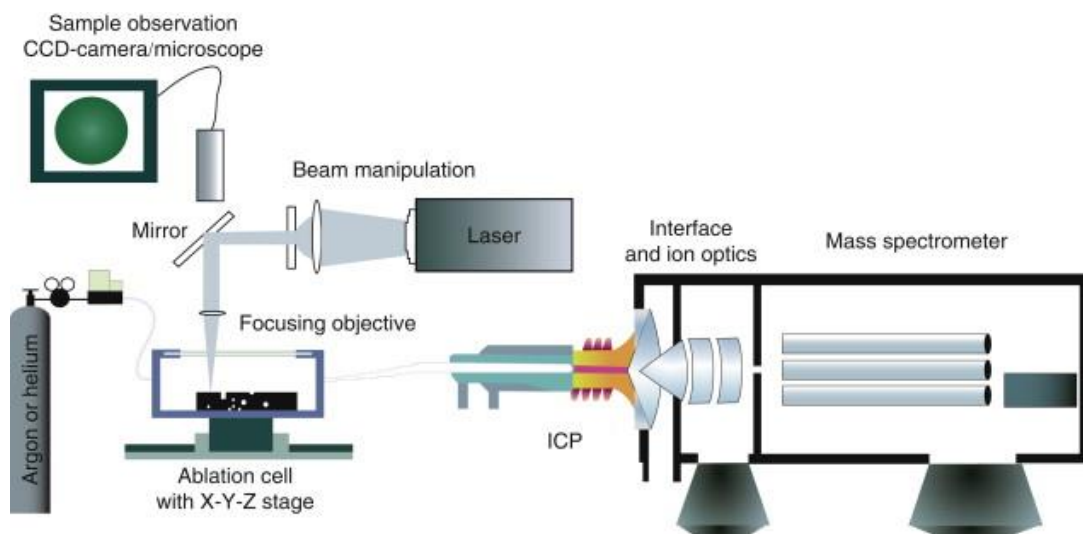


Figure 2 Schematic of an LA-ICP-MS system [10]

The ICP-MS system is usually used without the laser ablation system to conduct liquid ICP-MS measurements. This was also utilized in this work for validation purposes and a schematic can be seen in Figure 3. The ICP and MS part of this system is kept the same. However, the first part is exchanged with a sample introduction system for liquids consisting of a nebulizer and a spray chamber, which is used to create very small liquid droplets that form an aerosol which is then introduced into the plasma [12].

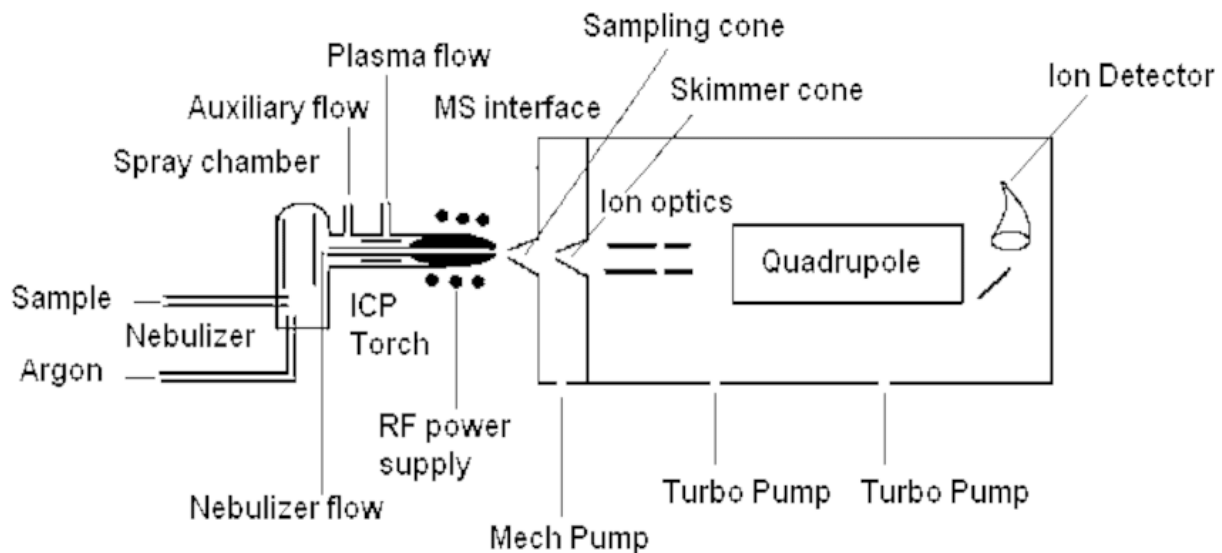


Figure 3 Schematic of a liquid ICP-MS system [11]

An autosampler can be connected to the system to decrease the workload as well as increase the consistency of the measurements. Liquid ICP-MS offers very low detection limits, fast measurements, and can be used to analyze a large number of different samples [12]. However, solid samples must be dissolved in a very laborious process before this method can be applied, which is not always possible. The sample is also destroyed in the process and a high amount of solvent needs to be utilized to prepare everything for the measurements. However, the largest drawback of this method is the inability to investigate small sections or areas of the sample in the micrometer range. Only bulk information is acquired [2].

## 2.1.2 Laser

The used laser plays a crucial part as a key component in the LA-ICP-MS system and is needed for the ablation of the targeted region of a sample material. Pulsed flashlamp pumped solid state Nd:YAG lasers are the most used type of laser for this method and are operated in the Q-switching mode [15].

For light amplification to occur it is necessary that the number of electrons in higher energy states ( $E_3$ ) is higher than the number of electrons in the ground state ( $E_1$ ). This phenomenon is called a population inversion and can be achieved in neodymium ions in the laser cavity through the use of an optical switch. This switch only opens when the maximum population inversion is reached and is called “pumping” [16].

A lamp which emits at the absorption level of Nd:YAG is needed for this pumping process to work. Two common lamps for this are the krypton flashlamps and xenon lamps, with the former being more efficient at low current densities [17].

The fundamental wavelength of a Nd:YAG laser is 1064 nm. However, to penetrate materials such as polymers efficiently, shorter wavelengths of 266 or 213 nm are required. Those are obtained through harmonic generation, which is based on the passage of a high intensity light beam through a birefringent crystal. The frequency of the oscillation of the material caused by the laser leads to the emission of light. This emission only happens in small electrical field strengths and only if the light intensity reaches an energy level similar to the binding strength of the electron. This causes non-linearity which leads to the production of overtones. Those overtones have frequencies that are multiples of the base frequency, hence the emission of wavelengths at 266 or 213 nm for the Nd:YAG laser. Other wavelengths are also possible, such as 532 and 355 nm, but are not relevant for this work [17].

A schematic of a Nd:YAG laser can be seen in Figure 4. The crystal consists of an Yttrium Aluminum Garnet (YAG) matrix doped with  $\text{Nd}^{3+}$  ions. The flashlamps are in positions parallel to the crystal and both are placed in a highly reflective cavity with mirrors placed on both ends to enhance the light absorption. The created laser pulse is directed through a partially reflective mirror into a fiber optic cable, which leads to a mirror that reflects the laser beam through a focusing lens onto the sample material. The laser is stationary during the whole process, with the workpiece instead being moved around on a X-Y stage [18].

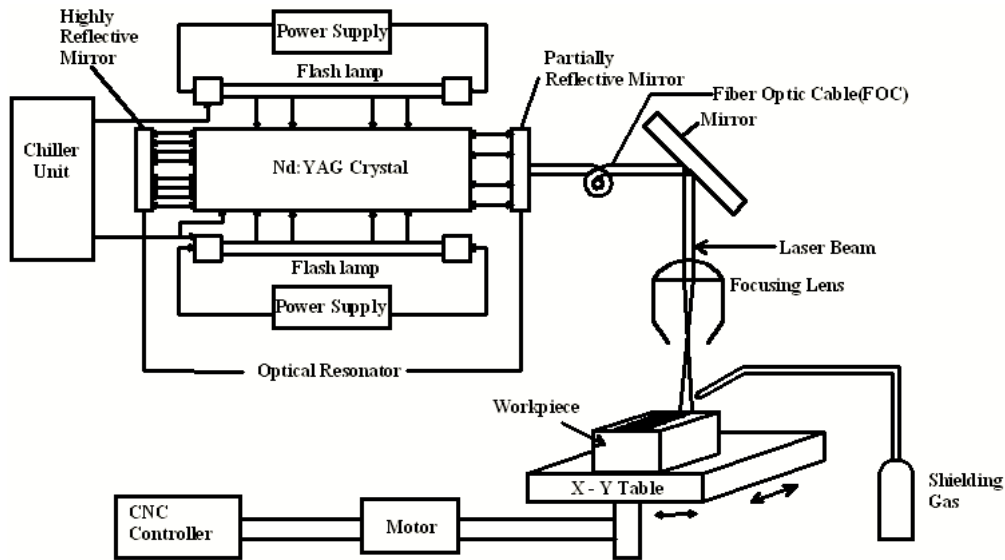


Figure 4 Nd:YAG laser system schematic [18]

### 2.1.3 ICP

The ablated sample aerosol is transported to the ICP via a constant Helium or Argon gas flow. A schematic of the ICP can be seen in Figure 5. It consists of 3 concentric quartz tubes and a water-cooled induction coil.

- The innermost tube is used to introduce the sample aerosol into the plasma generated by the induction coil.
- Auxiliary gas, which has the same composition as the plasma gas (Argon), is passed through the second tube to guide the aerosol into the central part of the plasma.
- The outermost tube is used for the transport of coolant gas (Argon) to prevent the tubes from melting as well as additional guidance of the sample aerosol to the plasma.

A magnetic field is generated by the rf current at a constant power of 1.2 to 1.3 kW with a typical maximum power of 2.5 kW in the induction coil. Seeding the Argon gas with energetic electrons results in the formation of plasma which is trapped by the magnetic field. The generated Plasma is self-sustaining and maintained as long as the magnetic field strength is sufficient. The temperatures in the plasma range from 10000 K to 6000 K leading to the atomization as well as ionization of the introduced sample aerosol in combination with a long plasma-sample interaction of 1-3 ms [20][21].

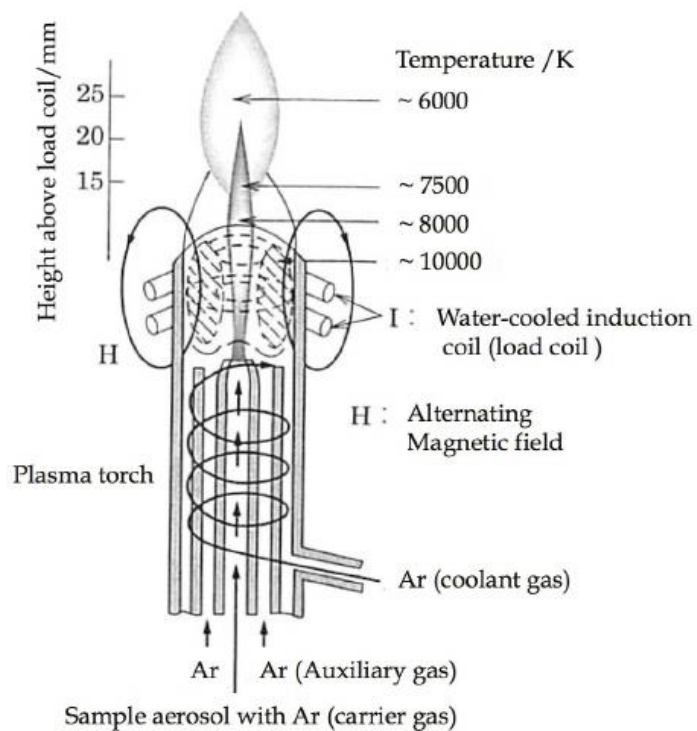


Figure 5 ICP schematic [19]

## 2.1.4 MS

A quadrupole mass spectrometer was used for detection in this work and will be discussed below. However, there are other options, namely the sector field as well as the time-of-flight mass spectrometer. All three function by separating the ions generated in the ICP by their mass to charge ratio ( $m/z$ ) [22].

The quadrupole mass analyzer consists of four metal rods of cylindrical shape which are placed parallel to each other. A current is applied to opposing rods, which are connected and have the same polarity. The applied voltage generates an electrical field which prohibits all ions from passing through the middle path between the rods except specific ions with a specific  $m/z$  ratio (Figure 6). Adjusting the voltage changes the pass-through  $m/z$  ratio which allows for exact and very quick scan rates. A detector is placed at the end of the path, which is usually an electron multiplier. Other options are microchannel plates, post-acceleration, and conversion dynodes as well as focal plane detectors which all convert the ion current into a countable signal [22]. The functionality of an electron multiplier is explained next.

The initial ion hits a dynode inside a vacuum chamber which leads to the ejection of an electron. This electron sets free more electrons through secondary electron emission by hitting another dynode. The newly released electrons repeat this process to generate multiple times the initial number of electrons depending on the  $m/z$  of the ion. This process massively intensifies the signal [22].

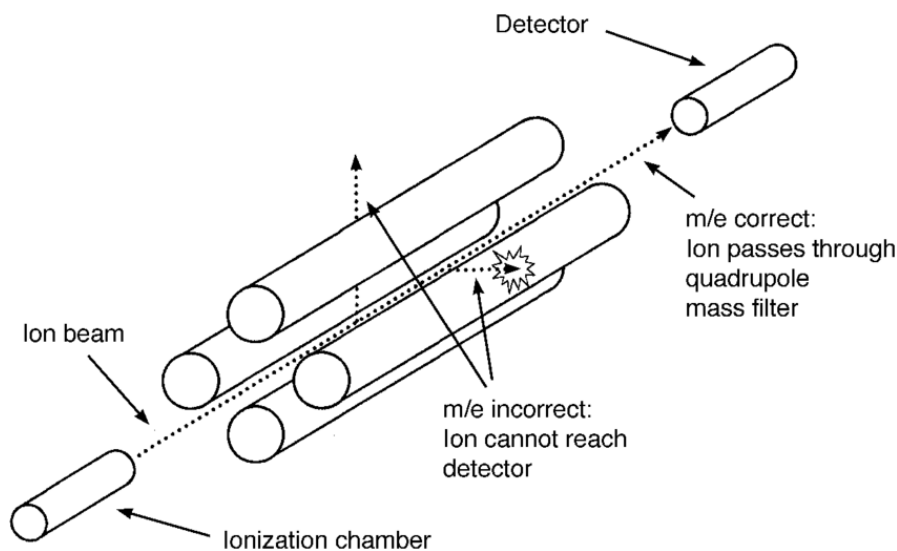


Figure 6 Quadrupole mass spectrometry schematic [23]

## 2.2 Quantification Methods for LA-ICP-MS

The quantification of analytes in the investigated sample is met with a plethora of problems that need to be solved, like non-stoichiometric effects during vaporization or problems with the transport of the ablated aerosol into the ICP, which are tied to the ablation behaviour of the material, the particle size, or material composition [25]. Those problem are usually solved through mundane means like changing the tubing, transport gas, or laser intensity but can also depend on the matrix of the investigated material, which makes standards with similar properties a requirement to achieve comparable efficiency.

A function needs to be available to correlate and ultimately evaluate the measured signal with the concentration in the sample material [25]. Elemental fractionation, and material-based matrix effects [26] make it a strenuous process to acquire such a function, which is often combined with the acquisition of a matrix-matched certified reference material (CRM).

### 2.2.1 Certified Reference Materials (CRM)

Certified reference materials are used for a wide variety of applications, such as standardized routine measurements in environmental and food chemistry, method validation, which is the topic of this work, proficiency tests, quality control and more [27]. Furthermore, all these operations also need to be validated, and assessed in their accuracy through different laboratories while offering comparable results. Having a CRM that is always the same no matter the location plays a critical role in this process [28].

CRMs, according to ISO Guide 17034, are defined as a “reference material characterized by a metrologically valid procedure for one or more specified properties, accompanied by a reference



material certificate that provides the value of the specified property, its associated uncertainty, and a statement of metrological traceability” [29].

An institution has to be accredited and certified to be able to produce and sell materials labeled as CRMs. The biggest and most important facilities are the National Institute of Standards and Technology (NIST) located in the USA, and the European Commission Joint Research Centre for Directorate F, Health Consumers and Reference Materials (JRC) located in Belgium. There are however many other institutions located around the globe that provide CRMs, such as National Measurement Institute Australia (NMIA) or Korea Research Institute for Science and Standards (KRISS) [28].

Despite the availability of a substantial amount of producers and sellers it cannot always be guaranteed to find the desired matrix matched CRM. This is especially true for novel materials such as polymers, which have unique and complex matrix compositions. Finding the right CRM with a similar or even the same matrix is nearly impossible due to most not existing. Those that do are only supplied in small quantities, which is made worse due to an increased demand leading to availability issues. Importing materials into specific regions is also not always possible due to import regulations and restrictions. This led to the development of other methods to circumvent the use of CRMs by creating in-house matrix matched standards or omitting the need to matrix match the calibration altogether.

### 2.2.2 In-house made standards for quantitative analysis

In-house made standards for analytical applications are commonly used as an alternative to CRM but have their own share of problems. Such alternatives can be tablets [30], microgrooves [31], micro-dried droplets [32], or materials used in production processes which have been analysed with alternative techniques, such as liquid ICP-MS measurements. This approach was used in this work to compare to the newly developed method.

The first method to be discussed is the creation of tablets as matrix matched standards measured separately from the actual sample. One such method was developed by Garbe-Schönberger et al. [30] without the need to add binders to the nano-particulate powder to create pressed powder tablets. This is however only applicable for powdered samples, thus for compact samples grinding is necessary, which could introduce additional error sources. The created tablets feature great cohesion and homogeneity but most importantly can be created out of powder made of natural rock, obtaining perfectly matrix matched standards in the process. However, this process takes multiple days to complete, is quite laborious, requires a high-power planetary ball mill, ultrapure water, and the samples undergo a freeze-drying step, which requires re-homogenization before being pressed into tablets [30].

The next method is based on the preparation of an aqueous standard without the need to match the matrix of the sample. However, this approach is a standard addition method that is directly applied to the surface of a solid sample and is based on the evaporation of a carrier solvent while leaving behind the solid standard. The described technique is called dried droplet evaporation and is used in quantitative polymer analysis [35] as well as in the quantification of catalytic materials [32]. The standard solutions are prepared with the desired elements dissolved in ultrapure water and applied to the surface with a pipette. The evaporation and complete dryness are achieved by inserting the sample in an oven [35]. This dried droplet evaporation approach is easily executed and is relatively fast but has major drawbacks, like the coffee ring effect [36], or reproducibility issues if not completely ablated due to “Hot Spots” of high sample intensity [37].

Micro-grooves or wells are a possible alternative to the dried droplet evaporation approach with a recent publication by Nischkauer et al. [31] using multiple parallel grooves with well-defined width and length as well as even spacing between grooves. The cavities were created by ablating grooves into poly (methyl methacrylate) (PMMA) microscope slides using the NWR 213 LA system [31], which is one of the laser systems used for this work. The aqueous standard solutions prepared beforehand were filled into the micro-array plates and analysed with an LA-ICP-MS system. The investigated sample material was blood with iron as the analyte, which was also filled into a separate set of micro-grooves and investigated with the same system. This setup creates the possibility to quantitatively evaluate liquid samples in a fast and simple way without the need for matrix matched standards [31]. Additionally, this method can be used for solid material as a standard addition method. The covered concentration range is however limited, and the absolute volume of the standard filled into the grooves is hard to determine. The actual determination of elemental ratios is simple and can be done as described in the publication by Horak et al. [43]

Chromatographic effects are usually compensated by ablating the entire droplet, this however creates the problem of pipetting exceptionally small volumes in the nanolitre range. It is also difficult to locate such a small drop on the substrate material with the camera of the laser. The grooves split up the sample droplet into many identical sub-samples in this range which increasing the visible area, which solves the aforementioned problems altogether. However, this method can only be applied to liquid or dissolved samples, only offers bulk information, and requires the preparation of microgrooves, which introduces additional risk of contamination [31, 33, 34].

Self-aliquoting wells can be utilised to mitigate some of the problems associated with this method and was recently done so by Horak et al. [32] by investigating nanoparticulate catalyst material. This method combined dried droplet evaporation with micro wells, which are created by ablating grooves into Makrolon® plates and filled with CRM. The access liquid has to be either wiped off or removed



with pressurized air. All liquid in the microwells evaporates within seconds due to the small amount contained within a groove. This makes the dried droplet arrays immediately ready for use omitting the oven step and concentrates the sample in small well-defined areas increasing the reproducibility and decreasing the coffee ring effect. However, the process is much more laborious, prone to contamination, only offers bulk information, and requires the solid sample to be transferred into the wells created on the Makrolon® plate [32].

### 3. Experimental

#### 3.1 Instrumental

The following instruments (Table 1) were used in this work. All ICP-MS measurements were conducted with an ICP-MS Thermo Fisher Scientific - "iCap Q", which utilizes a quadrupole system with a collision and reaction cell. The ablation of the sample material was accomplished through the use of two laser systems, a 213 nm Nd:YAG and a 193 nm Excimer laser, with the latter featuring much better sensitivity and precision. However, the former was used for the bulk of this work due to the 193 nm laser only being available during later stages of this work. An HTX TM-Sprayer was used to create the necessary standards with a well-defined concentration for the development of the standard addition method. The sprayer was also necessary for the creation of standards for reference measurements. The digestions for this purpose were conducted with an Anton Paar - Multiwave 5000 with Teflon vessels.

Table 1: Instruments.

	<p><u>ICP-MS Thermo Fisher Scientific - "iCap Q" [38]</u> Used for all ICP-MS measurements.</p>
	<p><u>Laserablation: ESL - "imageGEO193" [39]</u> Used for final measurements for optimal results.</p>

 A black laser ablation system with a central display showing a sample being analyzed.	<p><u>Laserablation: ESL "NWR 213" [40]</u> Used for majority of measurements.</p>
 A white HTX TM-Sprayer machine with a digital display showing '2.15' and a warning symbol.	<p><u>HTX TM-Sprayer [24]</u> Used to deposit standards onto the samples.</p>
 A red and white Anton Paar Multiwave 5000 microwave digestion system with a sample tray in front.	<p><u>Anton Paar - Multiwave 5000 with Teflon Vessels [41]</u> Used for sample digestion.</p>

A multitude of chemicals were used in the context of this work, be it as standards, solvents, or samples. The polystyrene, Kapton® and Nafion® polymer films were used as commercially available samples to test and optimize the newly developed standard addition method. ICP single element standards were later used as the standard of choice due to their high purity and availability. Early stages of this work utilized chemicals such as pyridine-2-thiol or disodium sulfate as standards. The carrier solvent for the spray process was created by mixing 18.2 MΩ Mili-Q water, which was made with a YYY-system and Barnstead D37 Hollow Fiber Filter, and propan-2-ol to create a 70 % high purity water. A list of all used reagents can be found in Table 2.

Table 2: Reagents

Chemical Name	CAS Number
Disodium sulfate	7757-82-6
Pyridine-2-thiol	73018-10-7
(Methanesulfonyl)methane	67-71-0
Propan-2-ol [Isopropanol]	67-63-0
Mili-Q Water (18.2 MΩ)	7732-18-5
Polyimide	58698-66-1
N-Methyl-2-pyrrolidon [NMP]	872-50-4
Poly(oxyethylene) [Polyethylenglycol]	25322-68-3
Polystyrene (19 μm)	9003-53-6
Kapton® (13 μm)	62929-02-6
Nafion® (27 μm)	31175-20-9
Nitric Acid (65 %)	7697-37-2
Hydrogen peroxide (30 %)	7722-84-1
ICP single element standards (S, Pb, Ag, Zn, Sn, In, Eu, Gd)	X

### 3.2 Method scheme

The following flowchart (Figure 7) depicts the necessary steps to determine the concentration of certain elements (in example Sulfur, Tin, Silver, etc.) in polymers.

The first step is the preparation of liquid standards through dilution. The range of concentration varies by element and was adjusted through multiple iterations to the concentration in the investigated sample. The standard solutions can range from  $\mu\text{g/g}$  to  $\text{ng/g}$ .

The prepared standards were then sprayed onto polymer film surfaces and Silicon wafers. The Silicon wafer samples were acid digested and measured with liquid-ICP-MS to determine the deposited mass per surface area ( $m_A$ ).

The element concentration of the polymer films was investigated by LA-ICP-MS measurements and subsequently evaluated with the  $m_A$  value previously obtained.

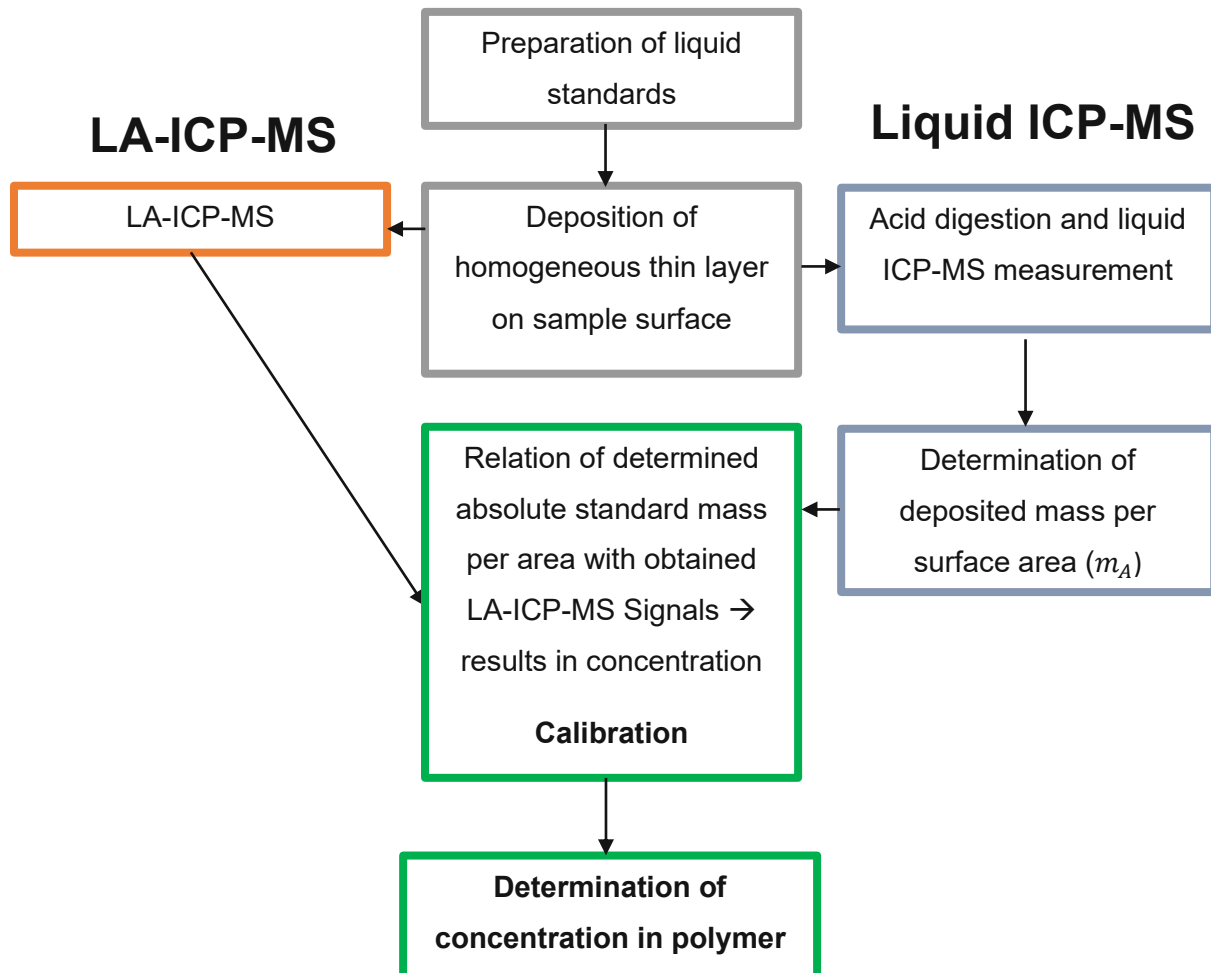


Figure 7: Method scheme

### 3.3 Standard preparation

The first standards were prepared by dissolving inorganic (sodium sulfate) and organic (Pyridine-2-thiol, methylsulfonylmethane) compounds in a Mixture of 70 % high purity water and 30 % isopropanol which was then sprayed on polymers with the HTX-TM-Sprayer. Although experiments did not lead to sufficiently good results because of a high degree of inhomogeneity of the standard as well as an uneven growth of the sprayed-on layer. The substrate layer also showed adhesion problems which resulted in the removal of large portions of the substrate during the ablation process. The used chemicals also show a tendency to grow in island like constructs which further decreased the viability of the method for precise measurements using a dot pattern (Figure 12) for the LA-ICP-MS. This led to the abandonment of this approach in favour of ICP standards in combination with a sprayed-on Carbon-based matrix. Polyethyleneglycol (PEG) was the chemical of choice for this due to its polymerization properties without any initiator or crosslinker. PEG creates evenly thick, homogenous films that show great cohesive stability during the laser process, meaning the sprayed-on layer stays in place and is not moved around. Only the targeted area of the coating is removed with adjacent areas being seemingly unaffected by the ablation process.

All subsequent standards were prepared in 70 % high purity water (30 % Isopropanol), a Polyethyleneglycol (10 kDa) matrix and a variety of ICP-standards (S, Pb, Ag, Sn, Zn, etc.). The analytes were spiked with Indium and the matrix was spiked with Europium. The In spiking was done to correct concentration errors caused by an



Figure 8: Kapton polymer film [42]

inhomogeneous distribution of the standard. Indium and the targeted standard must maintain a specific relation. Too little or too much indium indicates such an inhomogeneity and is hence corrected through the aforementioned relation. Europium as an internal standard works the same but forms a relation with the carbon in the sprayed-on PEG substrate layer. Errors by an uneven distribution can be corrected through this relation to prevent falsified results.

The substrates used were commercially available polymer films such as Polystyrene, Kapton® (Polyimide), and Nafion® with a focus on Kapton® (Figure 8).



Table 3: Standard preparation materials.

Substrates (sample)	Polystyrene, Nafion <sup>®</sup> , Kapton <sup>®</sup> (Polyimide)
Matrix	Polyethylenglycol (10 kDa)
Analytes	S, Pb, Ag, Sn, Zn, In, Eu, etc.
Solvent	30% Isopropanol

The standards produced covered a span of 1000 µg/g to 0.1 ng/g depending on the experiment and were tightened depending on the analyte element and investigated sample. Figure 9 is depicting a flowchart for the preparation of the liquid standards for spraying.

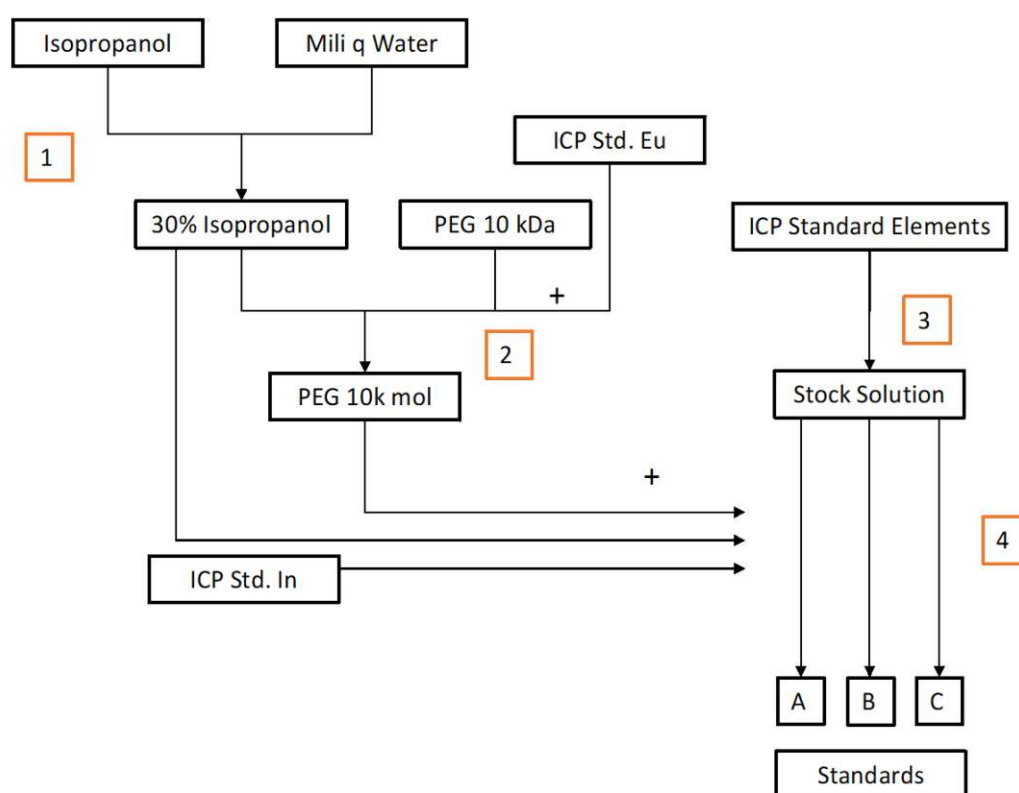


Figure 9: Flowchart for the preparation of the liquid standards for spraying.

- 1) Isopropanol was mixed with freshly dispensed MilliQ water to create a mixture of 30 % (v/v).
- 2) Polyethylenglycol (10 kDa) was then dissolved in the 30 % Isopropanol resulting in a 1% PEG solution in 30 % Isopropanol. The Europium was added as an internal standard to monitor the distribution of PEG on the sprayed substrate.
- 3) The third step required multiple ICP standards of the targeted analyte elements. Multielement stock solutions were prepared depending on the solvent being used in the ICP standards.
- 4) The stock solutions were then used to create spray solution standards for the HTX-spray by mixing 30 % Isopropanol, 1 % PEG, the stock solution, and Indium ICP standard. The endvolume

was chosen in such a way that the PEG would dilute to 0.5 % and the Indium to 1 µg/g. The Indium was used as an internal standard for the analytes for correcting distribution mistakes in the PEG matrix.

### 3.4 Polymer Film Substrate Preparation

The concept of applying standard addition requires at least the measurement of spiked and unspiked samples. In this work standard addition calibration was conducted by analysing multiple spike standard levels. However, to accomplish this with good consistency and on one sample substrate for all levels, it was necessary to manufacture masks. Those masks (Figure 10, Figure 11) were created using a 3D printer to ensure defined areas of 46 mm<sup>2</sup> of spray coverage on the sample surface. This is important to determine the deposited mass per surface area ( $m_A$ ) and subsequently the correct concentration in the investigated sample. Two types of masks were necessary for this. One for the polymer films (Figure 10) and one for the silicon wafers (Figure 11). All mask setups were prepared under a laboratory hood to minimize contamination risks.

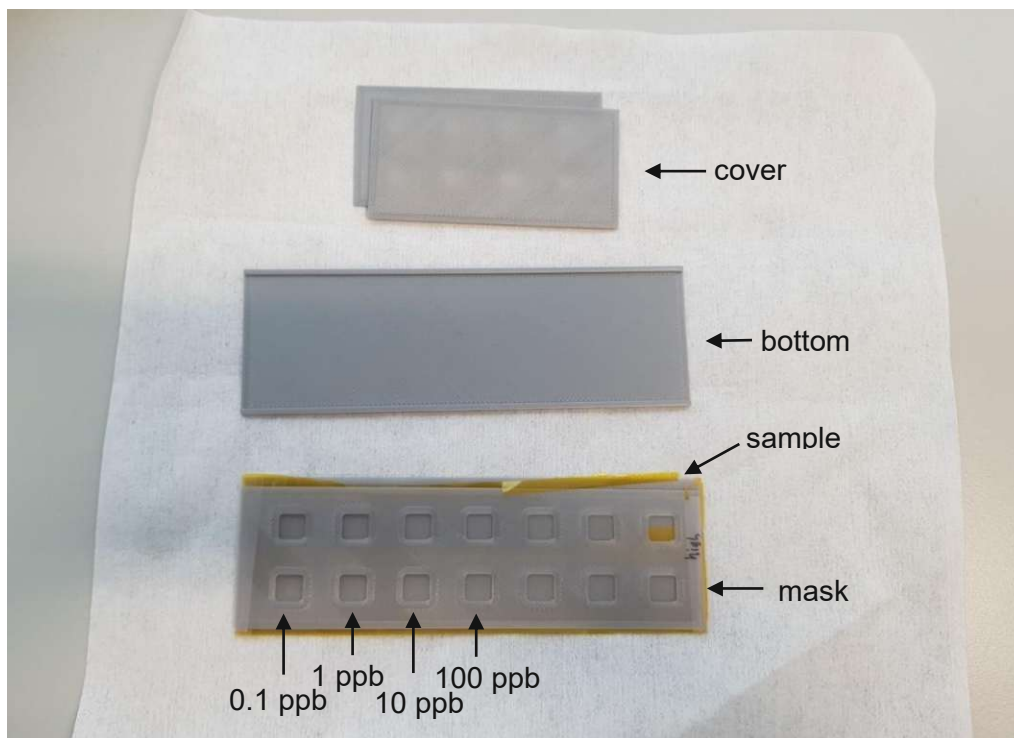


Figure 10: HTX-spray setup polymer.

The polymer setup consists of a bottom layer, the polymer film (substrate), the spray mask, and cover pieces to prevent contamination with other spray solutions. The polymer film and mask were separately attached to the bottom layer to ensure adequate stability during the spray pressure. The covers were used to cover the holes for other spray solutions or already sprayed sample surfaces. The spray order was chosen to start from the lowest concentration to the highest to minimise the contamination risk through other standards.



*Figure 11: HTX-spray setup wafer.*

The silicon wafer setup consists of a bottom layer with slots for the wafers, the wafers, a spray mask similar to the one used in the polymer setup, and polymer covers to prevent contamination during the spray process. It was crucial to have the same hole size for the polymer and wafer mask to ensure the sprayed area was the same. The slotsize for each wafer also needed to be precise enough to prevent the samples from moving due to the HTX-TM-Sprayers spray pressure.

### 3.5 LA-ICP-MS measurement

LA-ICP-MS line and spot measurements were conducted after spraying the samples with the prepared solutions. The line measurements were a crucial early step in the development process. Those were used to investigate the homogeneity of the deposited layers of analytes on the polymer surface but were quickly abandoned in favor of spot measurements to showcase the lateral resolution possibility of this method and because of the inability to completely ablate the targeted sample area with line scans. Most measurements were performed with an ESL "NWR 213" laser ablation system coupled with an ICP-MS Thermo Fisher Scientific - "iCap Q" system. The coupling of the two instruments was established using a 1.0-m-long PTFE tubing with an inner diameter of 1.0 mm. Later measurements were performed with an ESL "imageGEO193" laser ablation system coupled with an ICP-MS Thermo Fisher Scientific - "iCap Q" system due to the increased precision, intensity, and availability of it. The parameters can be found in Table 4.

Table 4: LA-ICP-MS parameters.

ICP-MS		LA	
Plasma power (W)	1400	He flowrate (ml/min)	650
Auxiliary gas flow rate (l/min (Ar))	0.8	Fluence (J/cm <sup>2</sup> )	1.5
Cooling gas flow rate (l/min (Ar))	13.8	Rep. Rate (Hz)	20
Make-up gas flow rate (l/min (Ar))	0.8	Spotsize (μm)	200
Measurement mode	Standard		
Measured isotopes	<sup>29</sup> Si, <sup>32/34</sup> S, <sup>64/66</sup> Zn, <sup>90</sup> Zr, <sup>98</sup> Sb, <sup>121</sup> Mo, <sup>107</sup> Ag, <sup>115</sup> In, <sup>120</sup> Sn, <sup>153</sup> Eu, <sup>158</sup> Gd, <sup>208</sup> Pb,		
Dwell time per isotope (ms)	10		

The sprayed polymer films were affixed to Si-wafers. This was done as an indicator for when the other side of the sample was reached. Measuring <sup>29</sup>Si in large quantities translates to a near complete ablation of the sprayed layer and polymer film, which was necessary for evaluation purposes.

The samples were then placed on a x-y-z stage inside the ablation chamber of the chosen laser system. An optical camera made it possible to focus the laser on the designated ablation zone on the surface of the sample. A spot size of 200 μm (d) was chosen and kept at this value. The vertical and horizontal distance between spots (x and y) were customizable parameters for the spot pattern as seen in Figure

12. The horizontal spacing for the line measurements was adjusted by increasing or decreasing the laser shot frequency and velocity at which the stage was moved. The pattern can be seen in Figure 12.

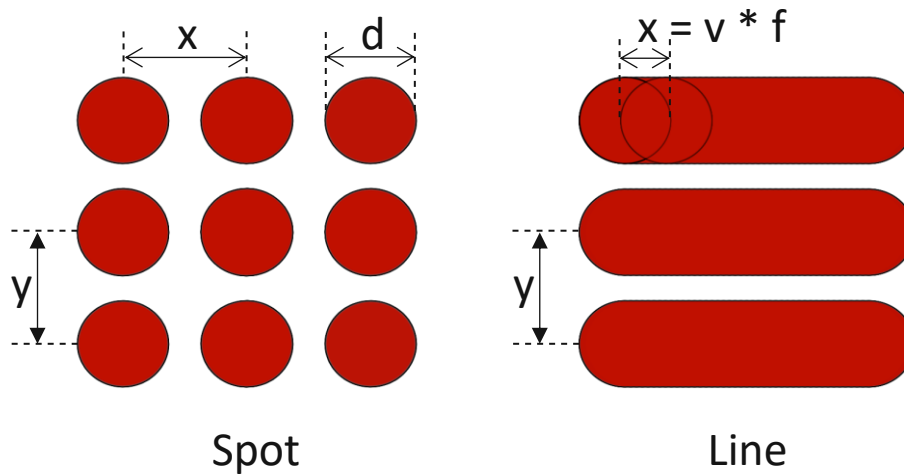


Figure 12 LA-ICP-MS Laserpatter for spot and line measurements. The horizontal and vertical spacing between laser shots are denoted as  $x$  and  $y$ . The laser spotsize  $d$  was kept at  $200 \mu\text{m}$  for all experiments. The horizontal spacing for the line pattern is adjusted by changing the stage velocity ( $v$ ) and the laser shot frequency ( $f$ ).

A NIST 612 reference standard was measured daily to ensure the LA-ICP-MS worked properly. Maintenance was also performed daily to maximize the  $^{115}\text{In}$  signal which utilized the autotune feature of the Qtegra data acquisition software (ThermoFisher Scientific).

$^{115}\text{In}$  and  $^{13}\text{C}$  were both used as internal standards.  $^{115}\text{In}$  was previously added as a constituent of the spray solution and was thus only present in the generated surface layer, while  $^{13}\text{C}$  is found in the polymer film. Indium was used to correct the analyte data for distribution errors, whereas the  $^{13}\text{C}$  was used to correct for the thickness of the film. Figure 13 shows a single-spot signal.

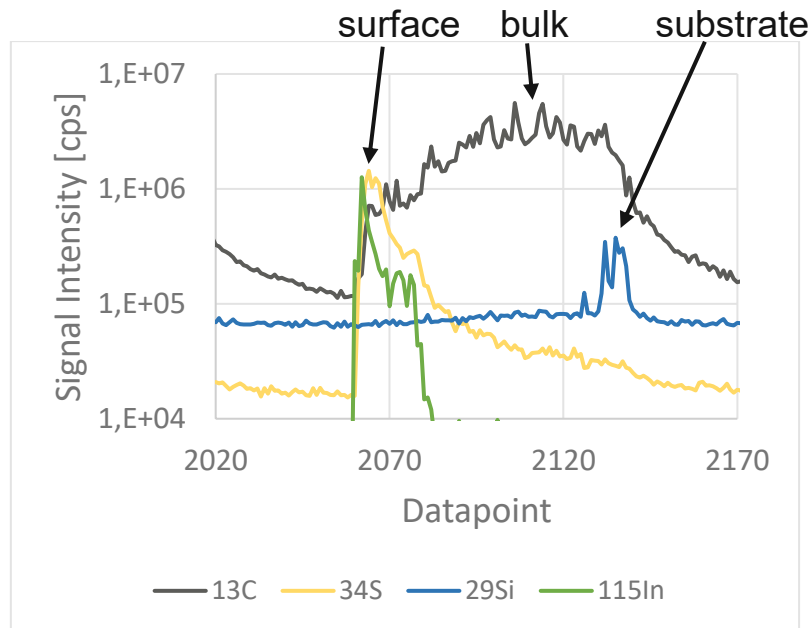


Figure 13 Single spot measurement; 1000 ppm Sulfur in spray solution; Indium internal standard; Kapton polymer;

For each spot measurement, three distinct observations areas can be assigned, the surface, bulk, and substrate. The surface area consists of the sprayed-on layer as well as the first few  $\mu\text{m}$  of the polymer film underneath. This is indicated by a first sharp increase in signal of Sulfur and Indium before any Carbon signal. The bulk indicated by large amount of  $^{13}\text{C}$  is the polymer film itself. The  $^{34}\text{S}$  signal gradually decreases until the background level is reached. An increase in  $^{29}\text{Si}$  signal indicates a near complete ablation of the sample film. It is crucial for the evaluation to ablate most of the sample, and it is also very important to wait long enough in-between spot measurements to flush out any leftover analyte or internal standard.

The isotopes measured in further experiments can be found in Table 4.

### 3.6 Microwave-assisted acid digestion and liquid ICP-MS analysis

Microwave-assisted acid digestion was performed to determine the  $m_a$  (= area specific mass deposition of the standard) through analyzing the sprayed Si-wafer samples previously prepared (Figure 11). This step was crucial in determining the concentration in the measured polymer films.

The second application was the validation of the LA-ICP-MS measurements through liquid ICP-MS measurements of acid digested polymer film samples. Kapton<sup>®</sup> needed to be cut into even pieces and weighted.

The sprayed wafers and cut Kapton<sup>®</sup> samples were transferred into separate Teflon vessels of the 20SVT50 microwave digestion rotor before adding 2.85 ml conc.  $\text{HNO}_3$  and 0.15 ml MilliQ to each. The temperature program used for the digestion can be seen in Figure 14. The maximum parameters for the vessels are limited to a pressure of 40 bar, a temperature of 300 °C and a volume of 50 ml. Higher pressure leads to pressure equalization and high temperature, or additional sample liquid can result in an uncontrollable increase in reaction gas which increases the pressure further, which is a safety hazard due to the risk of the vessel bursting. This should be avoided by monitoring the temperature in the vessels.

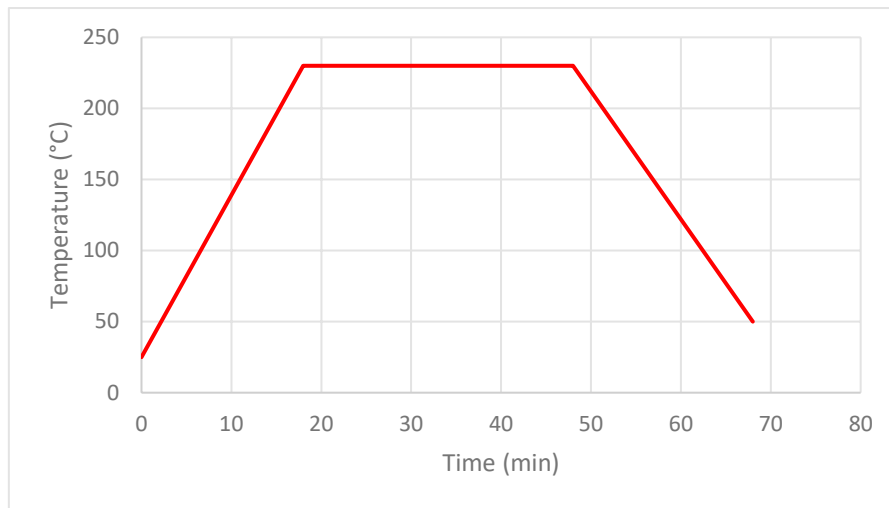


Figure 14: Microwave assisted acid digestion temperature profile.

The digestion solutions needed to be diluted with pure Mili-Q Water (18.2 M $\Omega$ ) to 10 % HNO<sub>3</sub> before conducting the liquid ICP-MS measurements to prevent any complications or damage to the machine. A set of 7 liquid standards covering the concentration range from 12.5 to 1000  $\mu\text{g/g}$  was prepared for each series of samples and needed to be measured multiple times throughout the process to monitor any possible drift of concentrations occurring over longer periods of time. Gadolinium (<sup>158</sup>Gd) was used as an internal standard and was introduced to the solutions with a concentration of 1  $\mu\text{g/g}$ .

The measurements were performed in standard mode without any reaction gas and Sulfur (<sup>32</sup>S) as the target analyte. The ICP-MS used for the liquid measurements was the same that was used for the LA-ICP-MS experiments. A self-aspiring PFA nebulizer intake system (Figure 15) with a flowrate of 400  $\mu\text{l/min}$  was used for the measurements. The autosampler model SC-2DXS with a FVA 6-way-valve system (Figure 16) was first used during the initial measurements and yielded great results. However, due to a malfunction of the instrument it was necessary to scrap that approach and measure all samples manually by introducing the tubing of the intake system into the samples and rinsing solution in between measurements. The system was tuned for the <sup>32</sup>S signal with the previously mentioned Qtegra data acquisition software. All ICP-MS parameters were kept the same as for the LA-ICP-MS measurements and can be found in Table 4.





Figure 15: Self-aspiring PFA nebulizer intake system

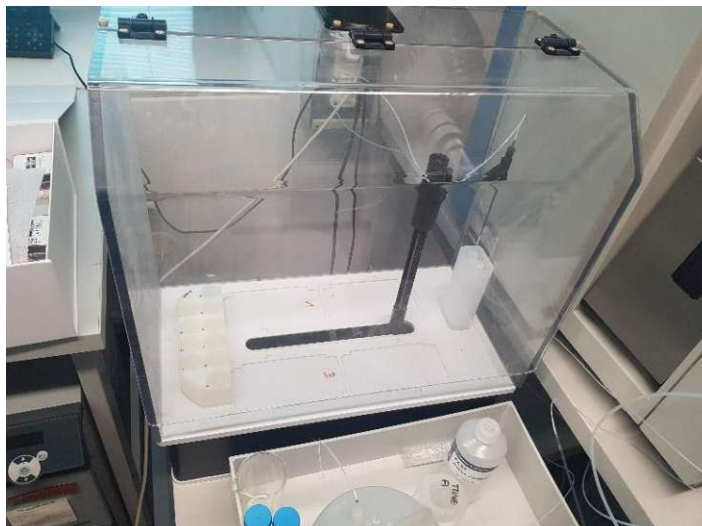


Figure 16: Autosampler model SC-2DXS with a FVA 6-way-valve system for the liquid ICP-MS measurements

## 4. Results and Discussion

### 4.1 Initial Experiments

The initial experiments were conducted to determine which compounds should be used as a Sulfur source and which solvent should be used for the spray purposes. Multiple aspects needed to be considered when choosing the appropriate materials for the experiments to obtain a sufficient degree of reproducibility. Most important of all being a homogenous surface distribution of the analyte to ensure consistent results between calibration measurements. The first analytes investigated were of inorganic and organic nature, specifically sodium sulfate, pyridine disulfide, and dimethyl disulfide were used. Multiple solvents such as water, isopropanol, and ethanol were used to dissolve and spray the analyte compound onto different polymer films (Figure 19). The surface sprayed with MiliQ as the carrier solvent shows an uneven distribution of the residues. This was further confirmed through LA-ICP-MS measurements, which have shown insufficient repeatability even on the same sample surface. This can be explained with the behavior the residues showcase. Larger crystals can be ejected from the surface when they come in contact with the laser, which happens due to an unknown mechanism. Conglomeration and growth of particles instead of the creation of new ones further decreases the homogeneity of the sprayed-on residues, which makes the matrix less approach unappealing. Mixing pure MiliQ water with pure isopropanol greatly improves the distribution of the residuals on the sample surface but was still found to be lackluster with a drift towards the sample edges (Figure 17, Figure 18) which was confirmed by performing spot measurements. The conglomeration problem was also not solved or improved upon, which is depicted in Figure 17 and Figure 19.

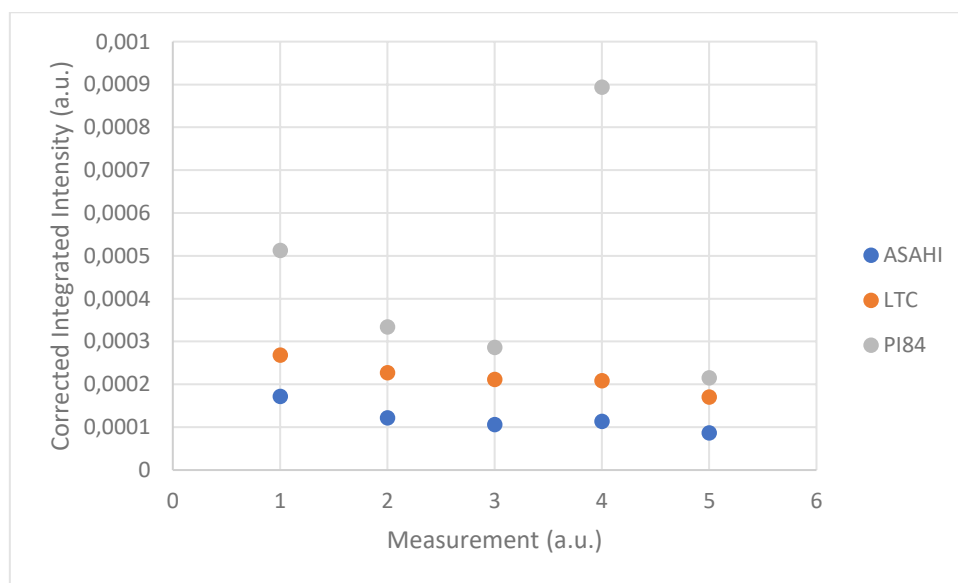


Figure 17 150  $\mu\text{g/g}$   $^{32}\text{S}$  LA-ICP-MS measurements on ASAHI, LTC, and PI84;  $^{32}\text{S}$  signal corrected for  $^{13}\text{C}$ ; background corrected; 1 middle of spray area; 5 edge of spray area (Figure 18);

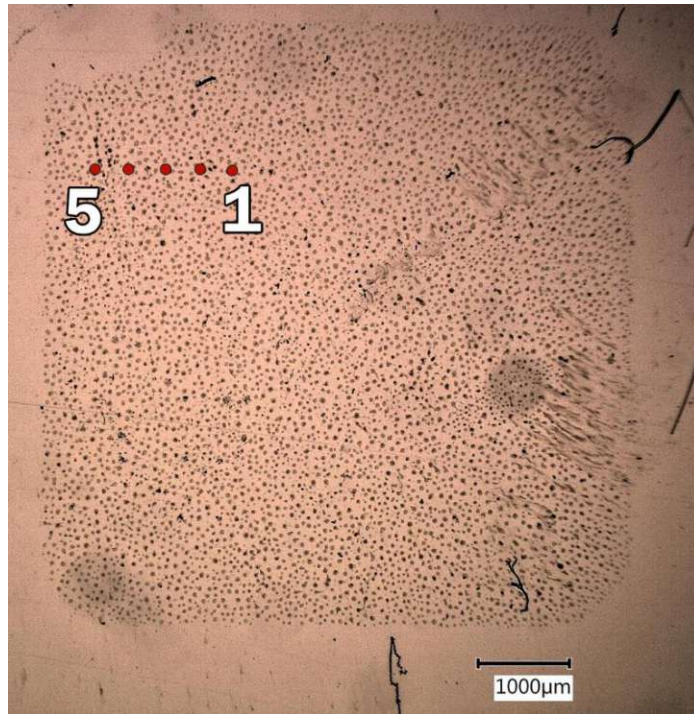


Figure 18 Exemplary spot-measurement area visualization

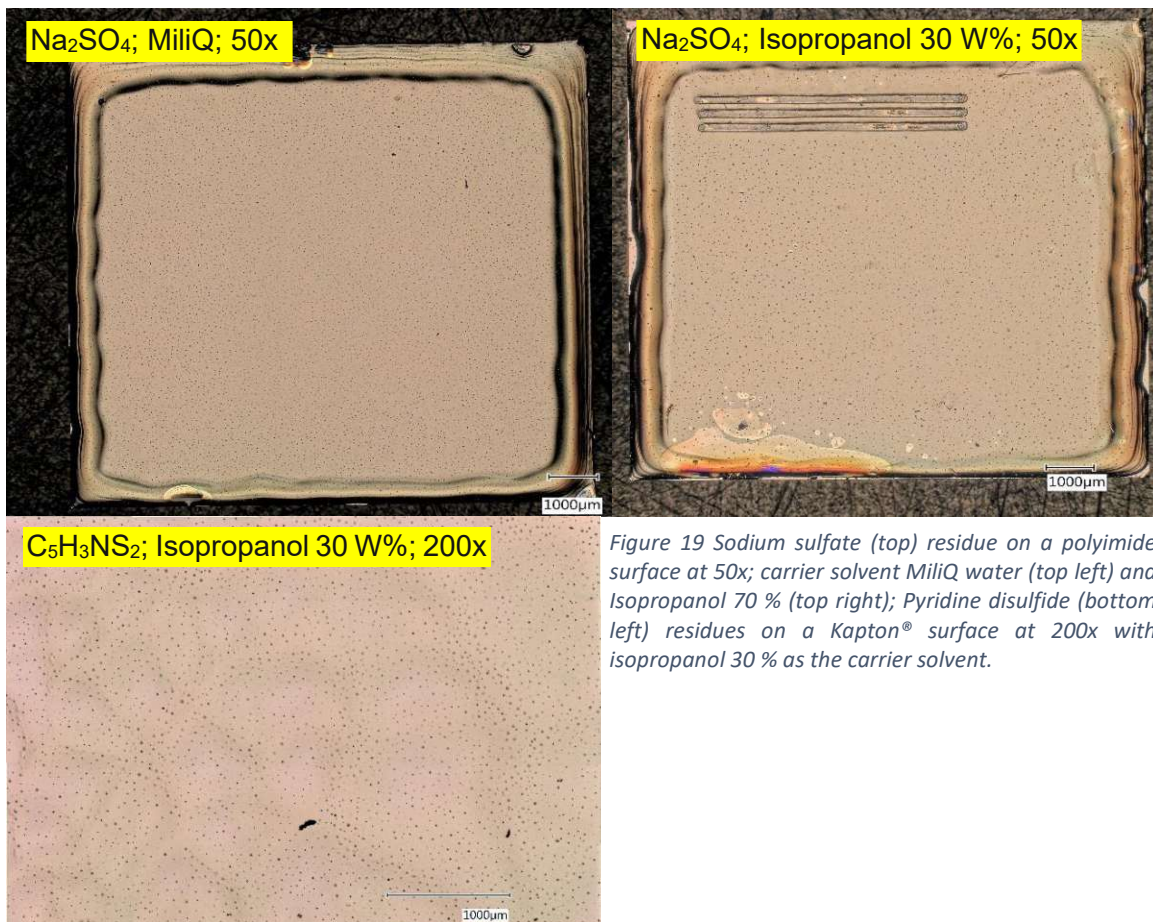


Figure 19 Sodium sulfate (top) residue on a polyimide surface at 50x; carrier solvent MiliQ water (top left) and Isopropanol 70 % (top right); Pyridine disulfide (bottom left) residues on a Kapton® surface at 200x with isopropanol 30 % as the carrier solvent.

The results of the previous experiments highlighted the need for either a matrix or monomer compound containing our analyte to ensure a homogenous distribution of the sample surface. This led

to the use of polyethylene glycol (PEG) in combination with isopropanol 30 % and a variety of ICP standards. The polymerization of PEG and simultaneous evaporation of our carrier solvent creates a relatively thin, homogenous layer on top of the sample, which contains the evenly distributed analyte. The HTX-spray parameters were optimized to ensure a homogenous deposition of the standards onto the samples. This was done by conducting a variety of experiments with different settings (Figure 20, Figure 21).

The first iterations were conducted with an organic compound without any PEG for experimentation purposes. Only one parameter was varied at a time, with spacing, cycles, and feed changing throughout the first few experiments. The final parameter to change were the spray cycles depicted in Figure 20.

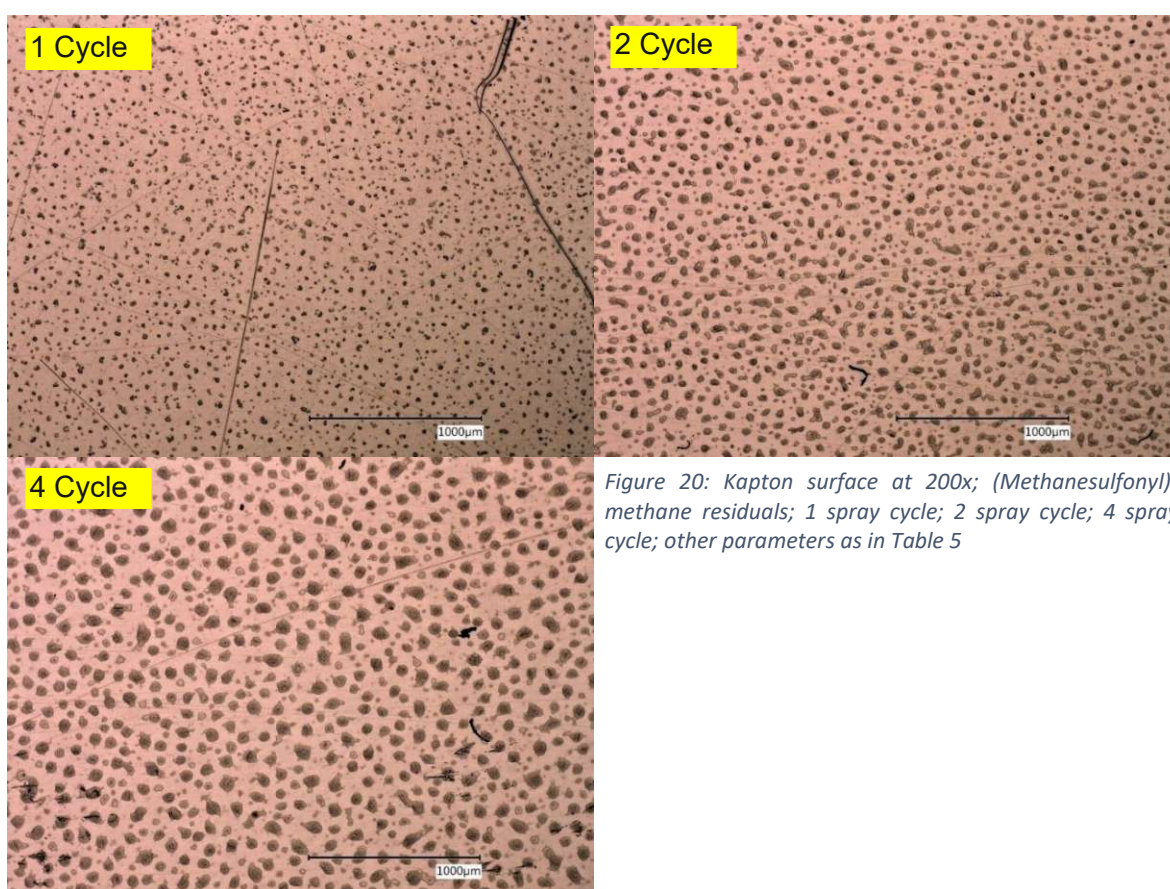


Figure 20: Kapton surface at 200x; (Methanesulfonyl)-methane residuals; 1 spray cycle; 2 spray cycle; 4 spray cycle; other parameters as in Table 5

This experiment highlighted the increased growth and conglomeration of residues based on the amount of spray cycles. Larger residues led to worse overall signal smoothness and reproducibility, with two cycles producing the best overall results. It is important to note that visual confirmation does not prove this. LA-ICP-MS measurements needed to be conducted to confirm any suspicion as discussed in chapter 3.5 LA-ICP-MS measurements.

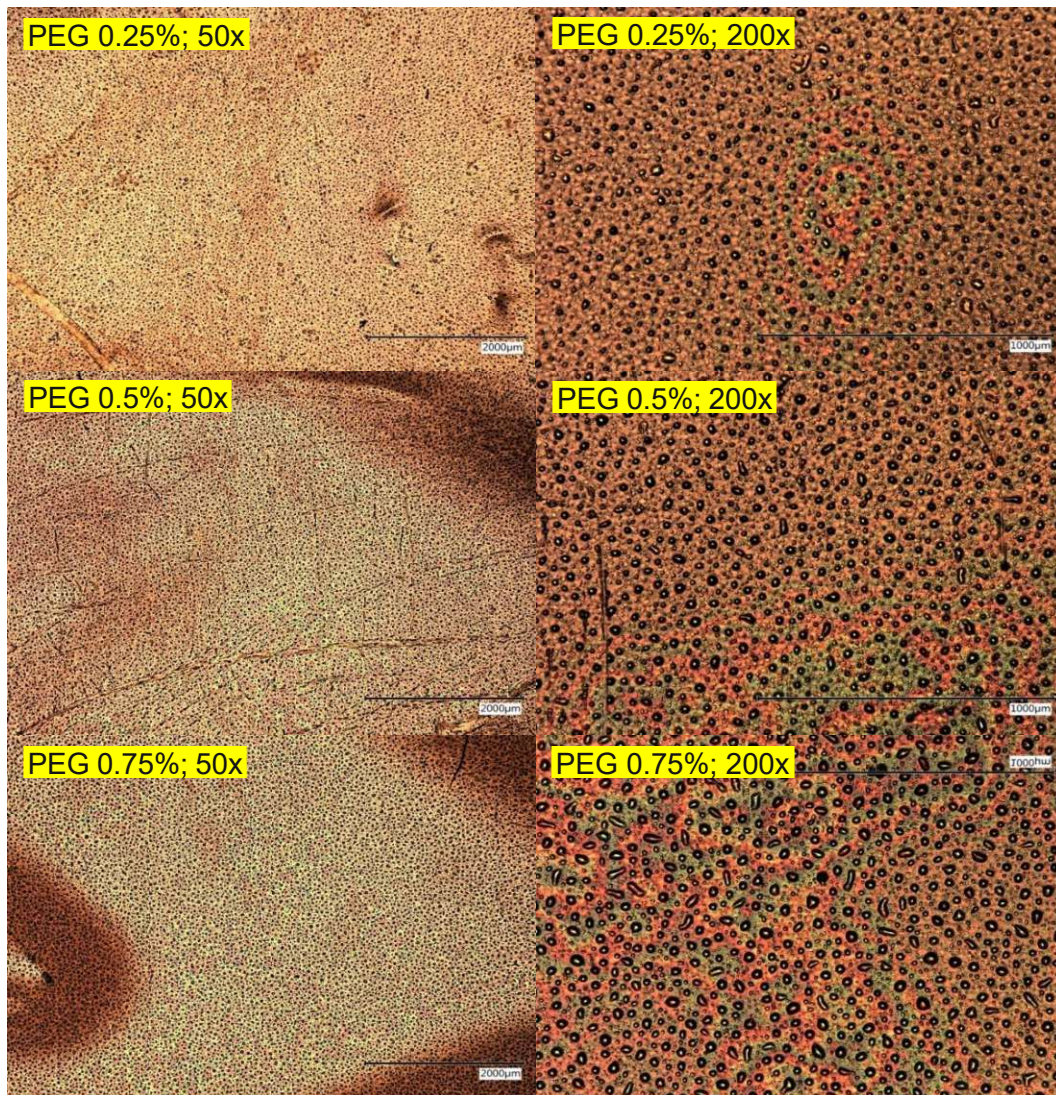


Figure 21: Kapton surface at 50x (left) and 200x (right); PEG 0.25 % (top); 0.5 % (middle); 0.75 % (bottom); other parameters as in Table 5

Figure 21 shows the influence of varying PEG concentrations on the residue distribution on a Kapton polymer film surface. Those experiments were conducted with the optimal HTX-spray settings (Table 5) previously defined. LA-ICP-MS measurements were performed to further investigate the signal smoothness which showed PEG 0.5 % as the best concentration at the chosen settings (Table 5).

Lower concentrations (0.25 %) created more plentiful but smaller residues. Those were ejected from the surface due to the intensity of the laser, which in turn had a bad effect on reproducibility.

Higher concentrations (0.75 %) led to bigger residues that were further apart which led to conglomeration and worse distribution overall, which in turn had a bad effect on reproducibility and signal smoothness.

All further experiments were conducted with the optimal HTX-spray settings (Table 5) and a PEG concentration of 0.5 %.

Table 5: Final HTX-spray parameters.

Line spacing (mm)	Spraying cycles (Cross pattern)	Auxiliary gas pressure (N2) (psi)	Scan Speed (mm/s)	Flow rate (ml/min)	Nozzle temperature (°C)
1	2	10	1000	0.03	45

It was also found that higher concentrations did not fall into a linear range anymore, which limited the investigation range. Lower concentration on the other hand were limited by the lowest possible detection limit of a specific element in the mass spectrometer.

Figure 22 shows a spot measurement series for Sulfur after optimizing the process for PEG and ICP standards as detailed before. A 1000 ppm Sulfur solution was sprayed on top of a Kapton® film which was then affixed to a Si-wafer surface. A sample surface zone was designated and covered in spots to perform multiple measurements in quick succession. The results show a homogenous distribution of the spray solution across the whole surface.

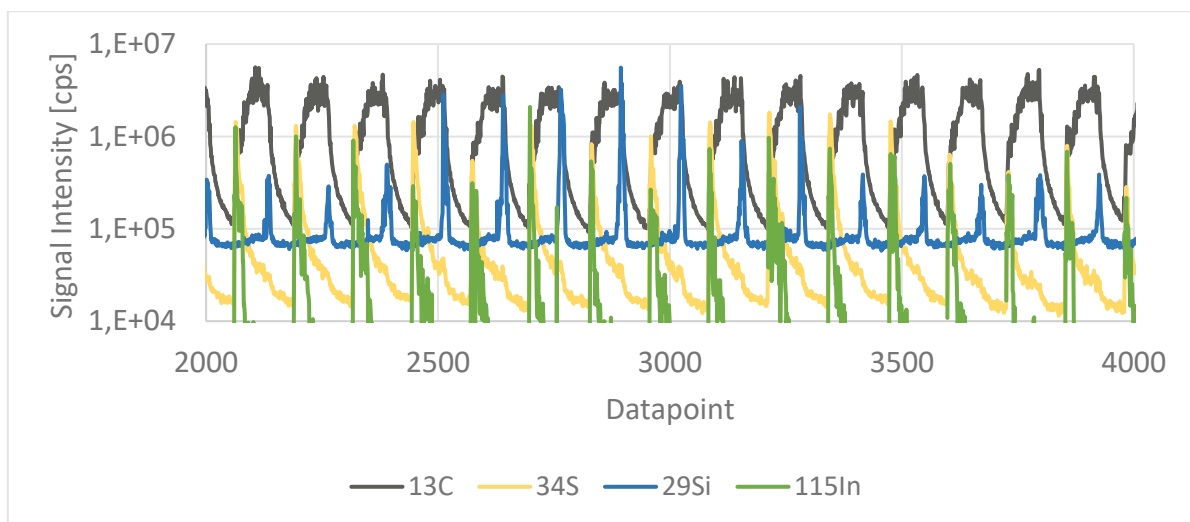


Figure 22 Multiple spot measurements; 1000 ppm Sulfur in spray solution; Indium internal standard; Kapton polymer; spray parameters as in Table 5;

## 4.2 Area specific mass deposition of the standard

The area specific mass deposition of the standard ( $m_a$ ) needed to be determined to calculate the concentration in the sample polymer film using the optimized conditions for the spray process.

The investigated analyte was Indium 10  $\mu\text{g/g}$  (In) in 10 %  $\text{HNO}_3$  with Gadolinium (Gd) as an internal standard. Eight samples were prepared as described in the chapter 3.6 Microwave-assisted acid digestion and analysis with liquid ICP-MS. The obtained signal was normalized for  $^{158}\text{Gd}$  and a standard calibration was measured during the liquid ICP-MS measurement series, which can be found in Figure 23. The measured S concentration in the range of 0 to 150  $\mu\text{g/g}$  resulted in a massive difference when compared to the acid digested liquid ICP-MS sample measurements. The raw data of the liquid ICP-MS measurements of the acid digested standard sprayed Si-wafers needed to be converted to the absolute mass of the standard in the spray solution applied to the wafer surface, which was done under consideration of the dilution of the measured sample. The first step required the calculation of the Indium concentration in the diluted digestion liquid of the sample, which resulted in a near perfect calibration (Figure 23).

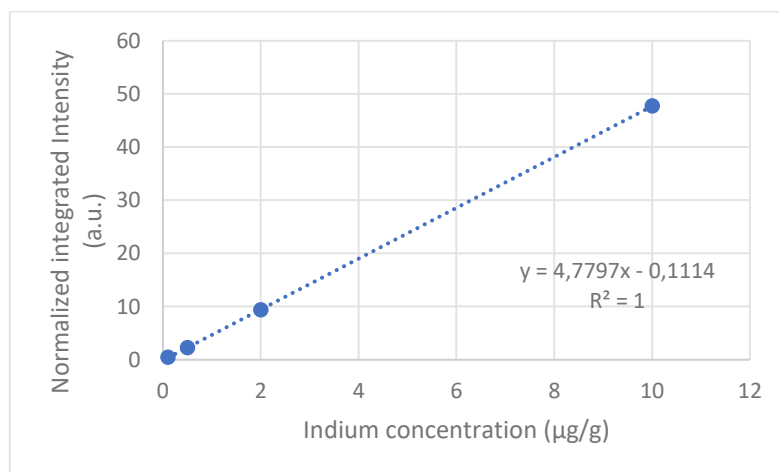


Figure 23 Indium standard calibration; liquid ICP-MS; normalized  $^{115}\text{In}/^{157}\text{Gd}$  (Table 13)

Equation 1 Liquid ICP-MS concentration calculation (Table 14)

$$c_{cal} = \frac{\text{normalized signal} - \text{intercept}}{\text{slope}}$$

The next step required knowledge about the exact area of deposition and dilution of the sample solution. The first value was obtained by using a defined mask with a  $46 \text{ mm}^2$  opening. This ensured a well-defined spray area. It was crucial to document the weight of each dilution step to calculate the dilution factor.

Equation 2 Area specific mass deposition calculation (Table 14)

$$m_a = \frac{c_{cal} * m_{ges} * m_{digest}}{m_{sample} * A_{depos}} * 10^{-9}$$

$c_{cal}$  ... Concentration of analyte in diluted solution [ppm]

$m_{ges}$  ... Mass of  $m_{sample}$  plus additional MiliQ needed to dilute to 10 % HNO<sub>3</sub> [g]

$m_{digest}$  ... Mass of sample liquid after digestion [g]

$m_{sample}$  ... Aliquote of sample liquid after digestion [g]

$A_{depos}$  ... Deposition area on wafer [mm<sup>2</sup>]

$m_a$  ... Area specific mass deposition [ppm\*pg/mm<sup>2</sup>]

The exact concentration in the spray solution was obtained by recalculating the concentration with the actual weight of each compound used.

$m_a$  ... Area specific mass deposition of the standard

$A$  ... Spot area

$d$  ... film thickness (13 μm)

$\rho$  ... polymer density (1,38 g/cm<sup>3</sup>)

$m_{STD}$  ... mass of the ablated deposited layer

$m_{poly}$  ... mass of the ablated polymer film

$c_{spray}$  ... concentration of analyte in spray solution

$c_{poly}$  ... concentration of analyte in polymer film

This resulted in a  $m_a$  of  $418 \pm 9$  ppm\*pg/mm<sup>2</sup> for 10.1 ppm In in the spray solution and needed to be normalized for 1 ppm.

$$m_{a,norm} = \frac{418 \pm 9}{10.1} = 4.13 \pm 0.92 \frac{pg}{mm^2}$$

Meaning we spray  $4.13 \pm 0.92$  pg/mm<sup>2</sup> for each 1 ppm analyte on top of the targeted surface.



### 4.3 Determination of concentration in the polymer film

To determine the actual concentration in the Kapton® polymer film, regular measurements needed to be conducted. A Sulfur standard series with Europium as an internal standard for the PEG was created, sprayed on top of the sample polymer film, and measured with 20 spot LA-ICP-MS measurements. The resulting signals were corrected for the added Europium and normalized for Carbon found in the polymer film. The obtained calibration (Figure 24) shows linear correlation with the intercept indicating native Sulfur content in the Kapton® polymer film. The signal of each standard concentration corresponds to the native Sulfur content in the measured sample and the sprayed on standard layer.

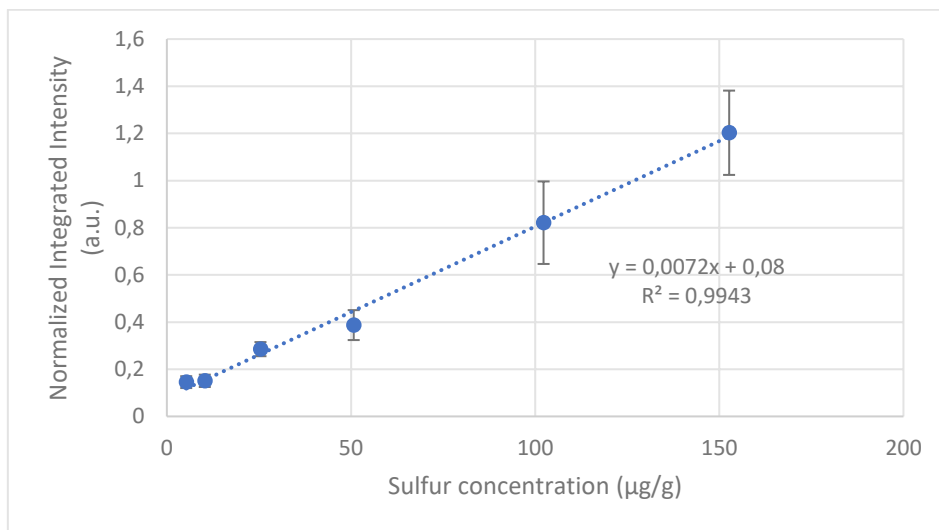


Figure 24 LA-ICP-MS Sulfur standard addition calibration; spray on Kapton®; Europium corrected; <sup>29</sup>Si normalized; imageGEO193 laser system (Table 15)

This calibration needs to be further modified by a factor  $f$ , which is calculated based on the  $m_a$  previously obtained. We assume 1 ppm of our analyte in the spray solution ( $c_{spray}$ ) used to create the deposited layer on top of the sample. The sample has a defined film thickness of 13 µm and a polymer density of 1.38 g/cm<sup>3</sup>. We further assume a constant spot area for the ablation laser. The ablated mass is the sum of the ablated deposited layer ( $m_{STD}$ ) and ablated polymer film ( $m_{poly}$ ). An illustration of the ablated sample can be seen in Figure 25.

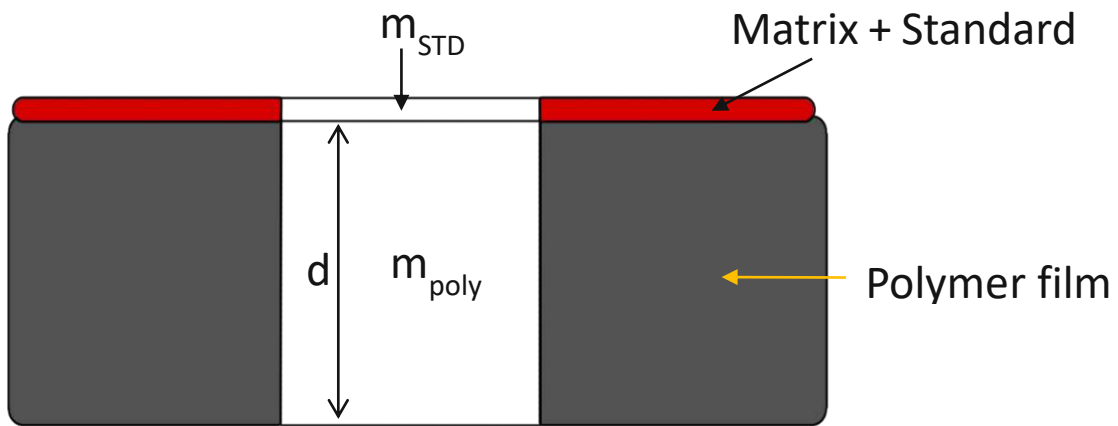


Figure 25 Illustration of an ablated sample;  $m_{STD}$  = mass of the ablated deposited layer;  $m_{poly}$  = mass of the ablated polymer film;  $d$  = film thickness

The ablated mass of the polymer and deposited layer can be calculated with the following equations.

Equation 3 Mass of the ablated polymer film

$$m_{poly} = \rho * V = \rho * A * d$$

Equation 4 Mass of the ablated deposited layer

$$m_{STD} = m_a * A$$

The concentration in the polymer film can subsequently be calculated without any influence of the spot area of the ablation beam.

Equation 5 Concentration of the analyte in the polymer film

$$c_{poly} = \frac{m_{STD}}{m_{poly}} = \frac{m_a * A}{\rho * A * d} = \frac{m_a}{\rho * d}$$

It was further assumed that the concentration in the spray solution must be modified by a factor  $f$  to correspond to the one in the polymer film. This factor needs to be isolated and can be used for all calibrations using the same carrier solution and spray parameters for the HTX-sprayer.

Equation 6 Calibration correction factor calculation

$$c_{spray} * f = c_{poly}$$

$$f = \frac{c_{poly}}{c_{spray}} = \frac{m_a}{\rho * d} = 2.32$$

The Sulfur concentrations of the previously obtained LA-ICP-MS Sulfur calibration (Figure 24) must be multiplied by  $f = 2.32$ . The modified calibration can now be used to calculate the correct concentration in the ablated polymer film, however it was first necessary to validate the results through another method.

## 4.4 Validation

The obtained LA-ICP-MS calibration can now be used to determine the Sulfur concentration in the polymer sample. 40 Blank measurements of the clean, unsprayed surface were measured and evaluated by normalizing the obtained signal for  $^{29}\text{Si}$ . Europium was not used to correct the signal because it was only used to correct for deposition irregularities of the sprayed PEG layer. To calculate the limit of detection (=LOD) and limit of quantification (=LOQ) the following formulas were used.

Equation 7 LOQ calculation

$$LOD = 3.3 * \frac{\sigma_{\text{intercept}}}{s}$$

Equation 8 LOQ calculation

$$LOQ = 10 * \frac{LOQ}{\sqrt{N}}$$

$\sigma_{\text{intercept}}$  ... standard deviation of the intercept of the calibration

s ... slope of the calibration

N ... number of tests (calibration points)

The calculated concentration of Sulfur in a 13  $\mu\text{m}$  thick Kapton<sup>®</sup> film based on the calibration is  $36.4 \pm 3.12 \mu\text{g/g}$  (Table 6), which is above the calculated LOD and below the LOQ for the calibration.

Table 6 Sulfur concentration in Kapton<sup>®</sup> film based on the LA-ICP-MS calibration; LOD and LOQ for calibration.

intercept	0.0032
slope	0.0800
Sulfur concentration ( $\mu\text{g/g}$ )	36.4
Sulfur concentration standard deviation ( $\mu\text{g/g}$ )	3.12
LOD ( $\mu\text{g/g}$ )	24.0
LOQ ( $\mu\text{g/g}$ )	98.0

Liquid ICP-MS measurements were chosen as the method of choice for validating the obtained results. The microwave assisted digestions of eight cut Kapton<sup>®</sup> polymer film samples were diluted and measured in standard mode without any reaction gas.  $^{158}\text{Gd}$  was used as an internal standard and the signal was normalized for it. The resulting calibration for the analysis can be seen in Figure 26.

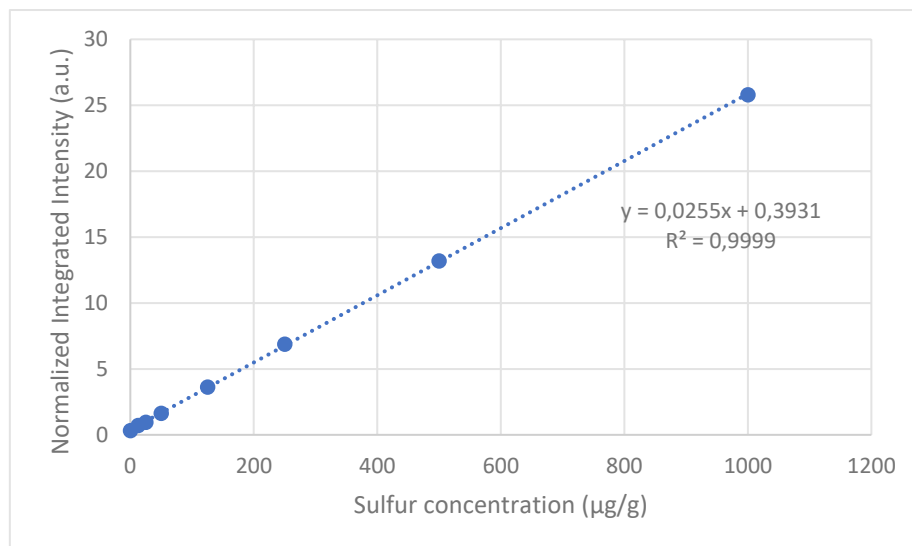


Figure 26 Liquid ICP-MS Sulfur calibration; normalized for  $^{158}\text{Gd}$  (Table 16)

The calculated concentration of Sulfur in Kapton® film based on the calibration is  $31.6 \pm 1.98 \mu\text{g/g}$  (Table 7), which is above the calculated LOD and below the LOQ for the calibration.

Table 7 Sulfur concentration in a Kapton® film based on the liquid ICP-MS calibration; LOD and LOQ for calibration.

intercept	0.0255
slope	0.3931
Sulfur concentration ( $\mu\text{g/g}$ )	31.6
Sulfur concentration standard deviation ( $\mu\text{g/g}$ )	1.98
LOD ( $\mu\text{g/g}$ )	13.5
LOQ ( $\mu\text{g/g}$ )	47.8

The results of the liquid ICP-MS and LA-ICP-MS are in good accordance with each other, which validates the LA-ICP-MS calibration method. Further measurements were conducted for other substrates and analytes to investigate the applicability of this quantification method.

## 4.5 Results polymer film

Sulfur was initially chosen due to its abundance in the investigated polymer film, but other impurities usually occur in low concentrations. Measurements were conducted to investigate possible analytes such as Zinc or Lead, which were found to be viable candidates. Calibration spray solutions were created as described previously and sprayed on top of a Kapton® film. The prepared samples were further analyzed with LA-ICP-MS measurements using the imageGEO193 laser system due to its increased precision and sensitivity. This improved the overall quality of the calibration and led to more precise results. The calibrations can be seen in Figure 27 and Figure 28 with both showing linear correlation with the intercept indicating native lead and zinc content in the Kapton® polymer film.

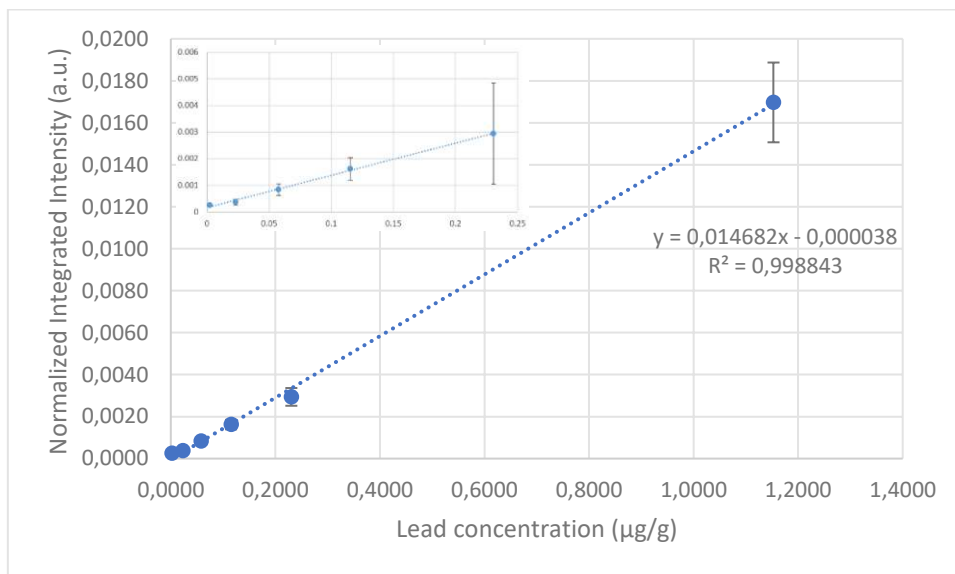


Figure 27 Modified LA-ICP-MS Lead calibration; spray Kapton®; Europium corrected; <sup>13</sup>C normalized; imageGEO193 laser system; (Table 17)

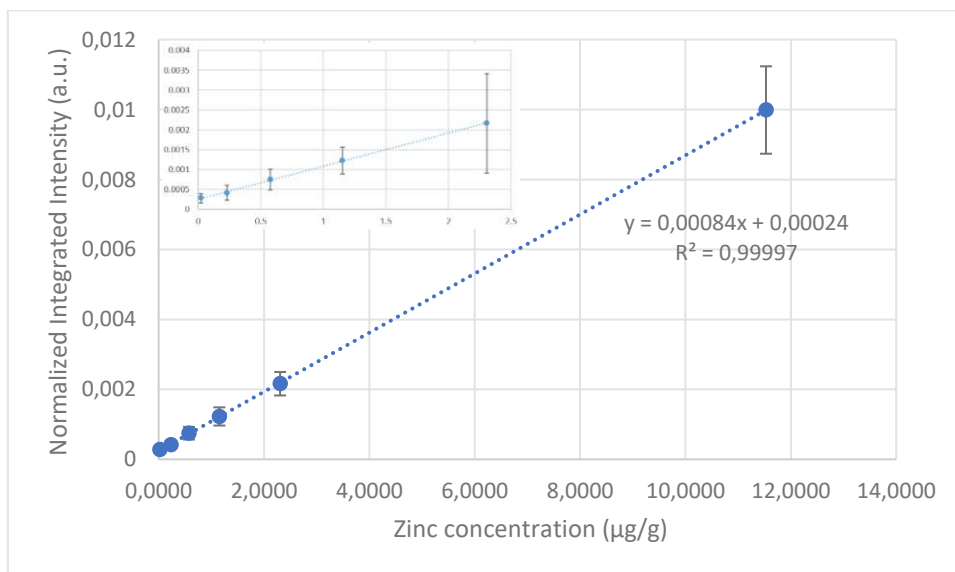


Figure 28 Modified LA-ICP-MS Zinc calibration; spray Kapton®; Europium corrected; <sup>13</sup>C normalized; imageGEO193 laser system; (Table 18)

The excellent calibrations were further used to calculate the concentrations of the chosen analytes and can be seen in Table 8. However, the obtained concentrations show a very high standard deviation, which hints at an inhomogeneous distribution of the analyte in the sample. Further, the calculated values are below the LOD (Equation 7) for the calibration which is below the lowest analyte concentration likely to be reliably distinguished.

Table 8 Lead and Zinc concentration in Kapton®

intercept	-0.000038	intercept	0.000242
slope	0.014682	slope	0.000845
Lead concentration ( $\mu\text{g/g}$ )	0.035	Zinc concentration ( $\mu\text{g/g}$ )	-0.0061
Lead concentration standard deviation ( $\mu\text{g/g}$ )	0.071	Zinc concentration standard deviation ( $\mu\text{g/g}$ )	0.8806
LOD ( $\mu\text{g/g}$ )	0.066	LOD ( $\mu\text{g/g}$ )	0.107
LOQ ( $\mu\text{g/g}$ )	0.271	LOQ ( $\mu\text{g/g}$ )	0.437

The same validation process as used for Sulfur was applied to Lead and Zinc. New Kapton® polymer film samples needed to be cut into even pieces and weighted before performing microwave-assisted acid digestions. The digested samples were prepared as described in chapter 3.6 Microwave-assisted acid digestion and measured with liquid ICP-MS. The calibrations show great linear correlation with an  $R^2$  of 0.9997 for zinc and lead as well as slopes of 0.0659 for zinc and -0.0851 for lead, which indicate great sensitivity for those elements.

Based on the determined element concentrations in the sample digests, the contents in the solid materials were calculated considering the dilution and intake of the measured solution. The calculated concentrations can be seen in Table 9. The 12 digested cut samples represent a much higher analytical volume than the 200  $\mu\text{m}$  spot measurements but still showcase a high standard deviation when compared with Sulfur. This is most likely not a methodological problem but tied to the investigated polymer film, hinting at a highly inhomogeneous distribution of the analytes in the Kapton®, which makes a validation of the LA-ICP-MS measurements impossible.

Table 9 Lead and Zinc concentration in Kapton®

intercept	-0.0851	intercept	0.0659
slope	3.018	slope	0.2786
Calibration range Lead ( $\mu\text{g/g}$ )	0 - 25	Calibration range Zinc ( $\mu\text{g/g}$ )	0 - 25
Lead concentration ( $\mu\text{g/g}$ )	1.05	Zinc concentration ( $\mu\text{g/g}$ )	2.95
Lead concentration standard deviation ( $\mu\text{g/g}$ )	0.717	Zinc concentration standard deviation ( $\mu\text{g/g}$ )	1.87
LOD ( $\mu\text{g/g}$ )	0.682	LOD ( $\mu\text{g/g}$ )	0.776
LOQ ( $\mu\text{g/g}$ )	2.58	LOQ ( $\mu\text{g/g}$ )	3.17

360 spot measurements of Kapton® film were conducted to investigate the homogeneity of the analytes in the sample. The results can be seen in Figure 29. The normalized Pb signal was further offset on the y-axis to better highlight the distribution of each measured analyte, with some measured spots showing an exceptionally high signal of the target analytes. There is, however, no correlation between the elements and their increased concentration. This further lends proof to the assumption of a completely random distribution of highly concentrated areas of Lead and Zinc in the investigated sample.

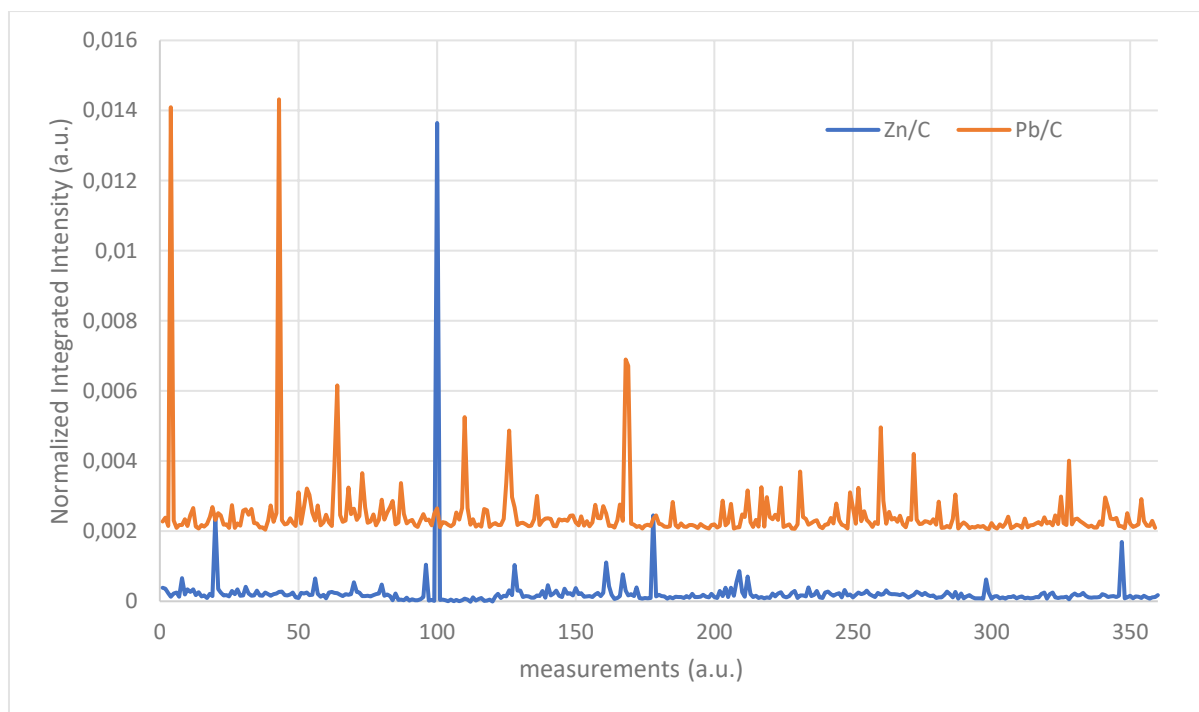


Figure 29 360 spot measurements of Kapton® film; Zinc and Lead; Carbon normalized; Pb/C y-axis offset by 0.002;

Liquid measurements offer bulk information in form of the average concentration in a large sample. However, LA-ICP-MS spot measurements only offer information of a small sample volume even at a

sample size of 360 and are not representative of the whole sample. Line measurements can be performed but do not compensate for the size difference between the analyzed volumes. This made a comparison of measurements of highly inhomogeneous samples nearly impossible, which in turn made a validation of the obtained LA-ICP-MS Zinc and Lead calibration with the liquid ICP-MS method impossible.

## 4.6 Other Polymer Substrates

Two other polymer films (Polystyrene, Nafion®) were used to test the calibration approach. Pb and Zn were both chosen as the analytes to investigate their behavior on another substrates. Those elements were chosen due to their possible occurrence in the chosen polymer films based on initial measurements with the LA-ICP-MS. Calibration spray solutions were created as described previously and sprayed on top of a Polystyrene and Nafion® film. The prepared samples were further analyzed with 40 LA-ICP-MS spot measurements for each concentration and blank using the ESL "NWR 213" laser system. The measured signal was Europium corrected and normalized for Carbon contained within the sample. The concentration of each analyte was adjusted based on the calculations described in chapter 4.3 Determination of concentration in the polymer film.

The resulting Zn and Pb calibrations for Polystyrene (Figure 30, Figure 31) show linear correlation in between 0.025 µg/g and 20 µg/g, with Pb showing exceptionally good results. Measuring low Zn concentrations resulted in the clustering of signals (Figure 30) when applied to prepared standard samples. This error can be attributed to a potentially high Zn concentration in the polymer film covering the very low signal for the ppb standard range, which is reinforced due to the increased intercept. This is further supported by high LOD and LOQ values (Table 10) due to the standard deviation of the blank measurements being very high. This is caused by a high degree of inhomogeneity in the sample for the investigated analytes, which further explains the high standard deviation.



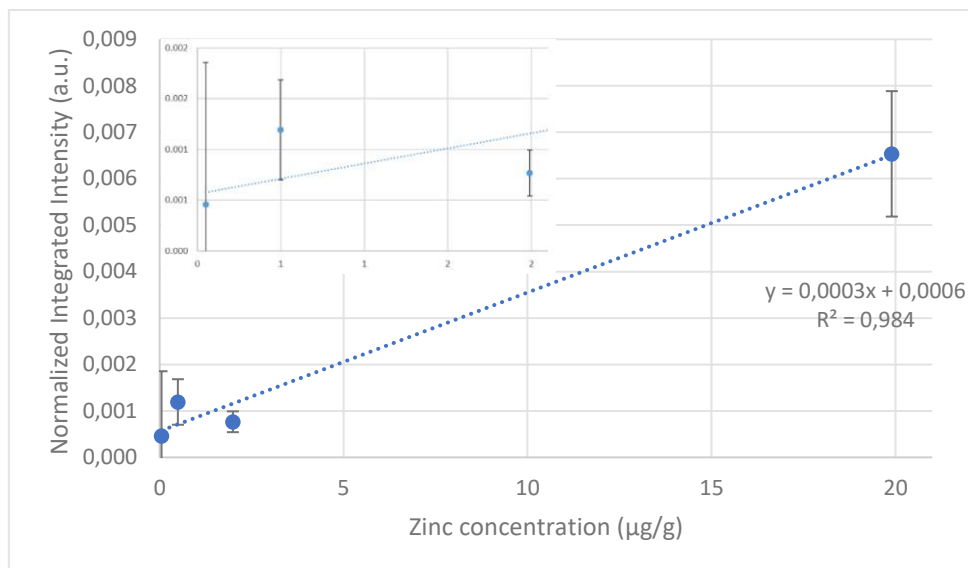


Figure 30 Modified LA-ICP-MS Zinc calibration; spray Polystyrene; Europium corrected; <sup>13</sup>C normalized; imageGEO193 laser system; close up (Table 21)

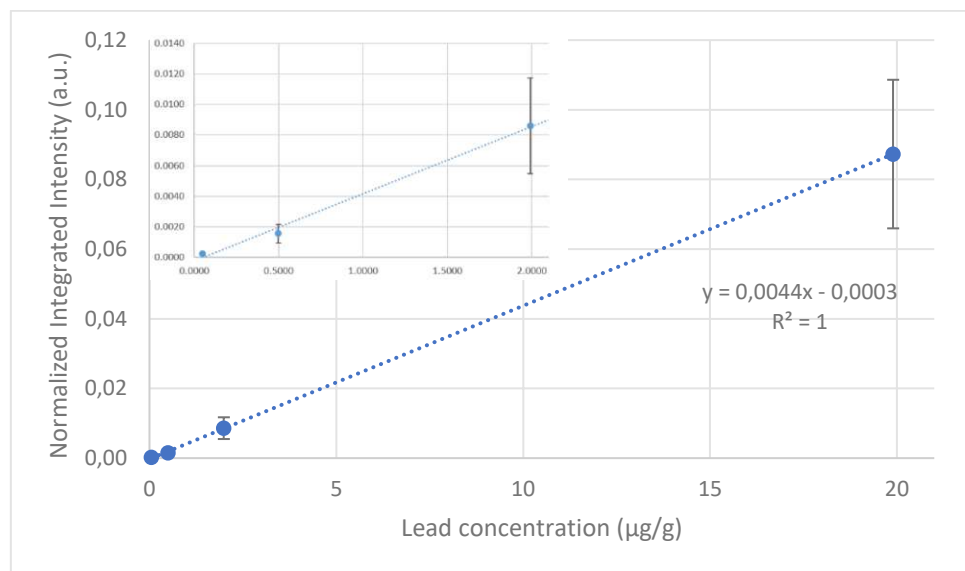


Figure 31 Modified LA-ICP-MS Lead calibration; spray Polystyrene; Europium corrected; <sup>13</sup>C normalized; imageGEO193 laser system; (Table 22)

Table 10 Lead and Zinc LOD and LOQ in Polystyrene

LOD Lead (µg/g)	0.371	LOD Zinc (µg/g)	6.01
LOQ Lead (µg/g)	1.51	LOQ Zinc (µg/g)	26.9

Liquid ICP-MS measurements were conducted for validation purposes but failed due to exceptionally low concentrations of the target analytes in Polystyrene.

The resulting Zn and Pb calibrations for Nafion® can be seen in (Figure 32, Figure 33) and show linear correlation. The relatively high intercept for Zn indicates native Zn content with the high standard deviations indicating inhomogeneity in the investigated sample. Pb however shows a negative intercept combined with a relatively high standard deviation for higher standard concentrations. This hints at no Pb being present in the sample, with the deviation being caused by Pb inhomogeneity in the sprayed-on layer. Another possibility is an incredibly inhomogeneous sample with no concentration in between pockets of Pb grains. The calculated LODs and LOQs (Table 11) further hint at inhomogeneity issues.

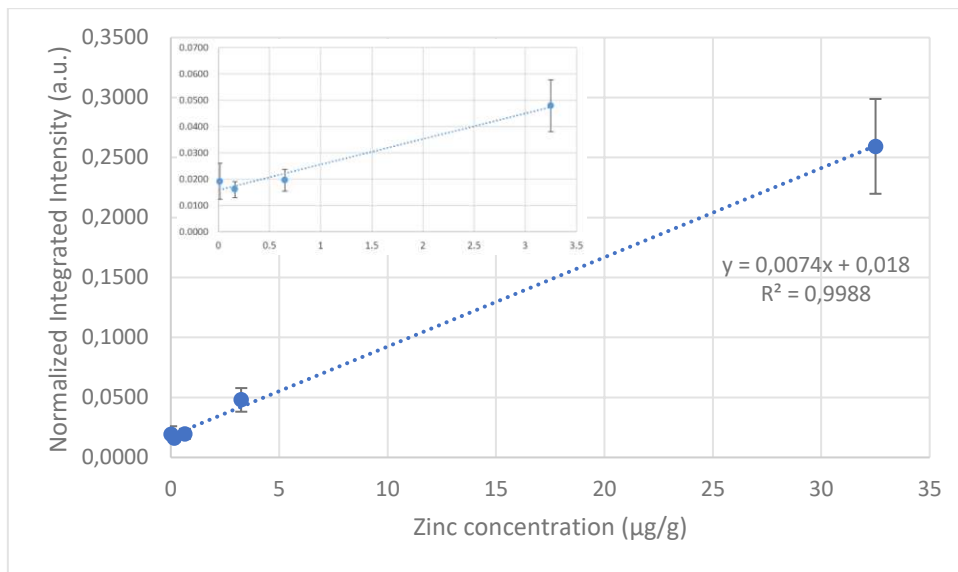


Figure 32 Modified LA-ICP-MS Zinc calibration; spray Nafion®; Europium corrected; <sup>13</sup>C normalized; imageGEO193 laser system; (Table 23)

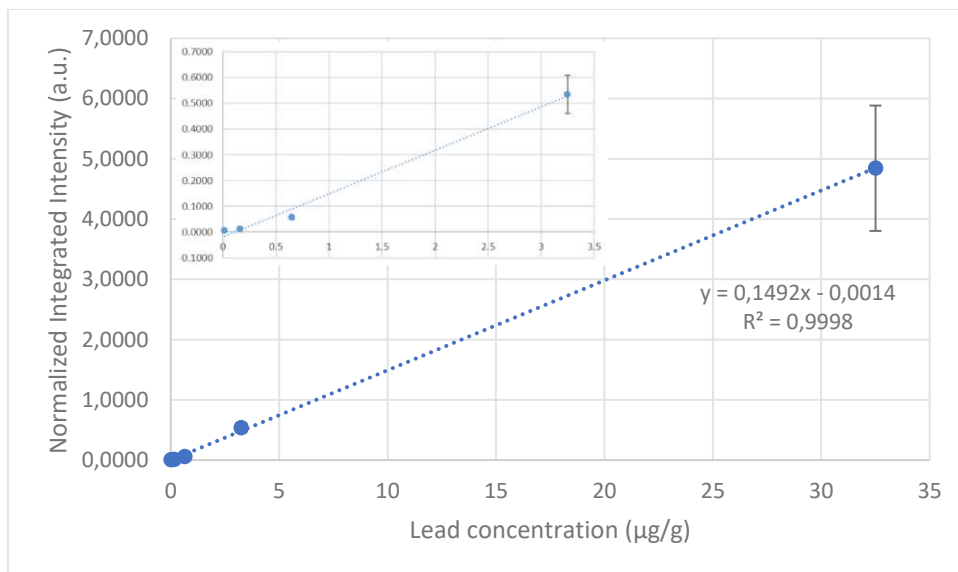


Figure 33 Modified LA-ICP-MS Lead calibration; spray Nafion®; Europium corrected; <sup>13</sup>C normalized; imageGEO193 laser system; (Table 24)

Additional spray solutions for Mo, Zr, and Sb were prepared and sprayed on a Nafion® film. The samples were analyzed with LA-ICP-MS measurements using the ESL "NWR 213" laser system. The obtained data was Europium corrected and normalized for Carbon contained within the sample. The concentration of each analyte was adjusted as described in chapter 4.3 Determination of concentration in the polymer film. The resulting calibrations (Figure 34, Figure 35, Figure 36) show linear correlation for the whole range. However, all calibrations show very high standard deviations for all standards which indicates an inhomogeneous distribution of the analytes in the measured sample. Furthermore, an increased intercept can be seen for Mo (Figure 35) which indicates the occurrence of this element in the Nafion®. High LOD and LOQ values (Table 11) make this assumption much more likely.

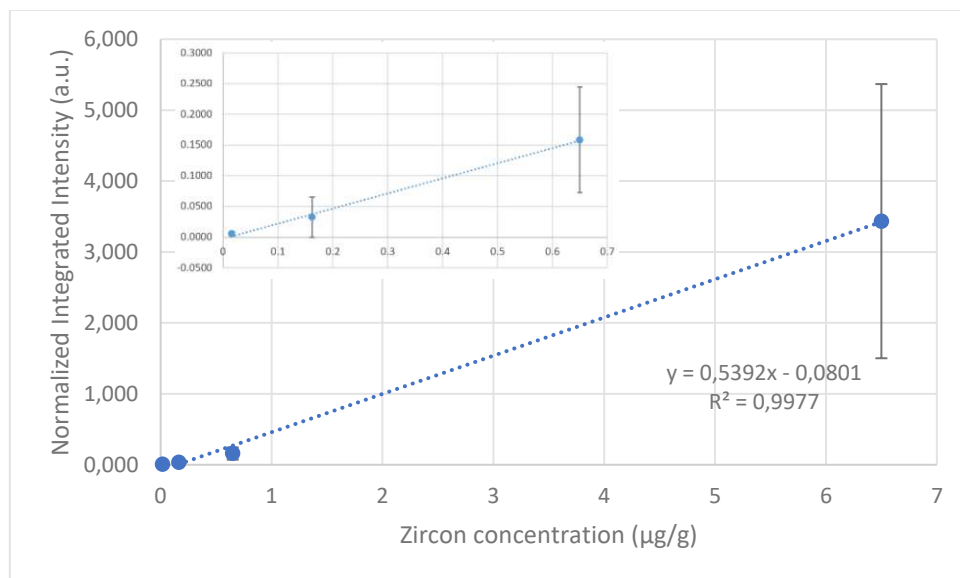


Figure 34 Modified LA-ICP-MS Zircon calibration; spray Nafion®; Europium corrected; <sup>13</sup>C normalized; imageGEO193 laser system;(Table 25)

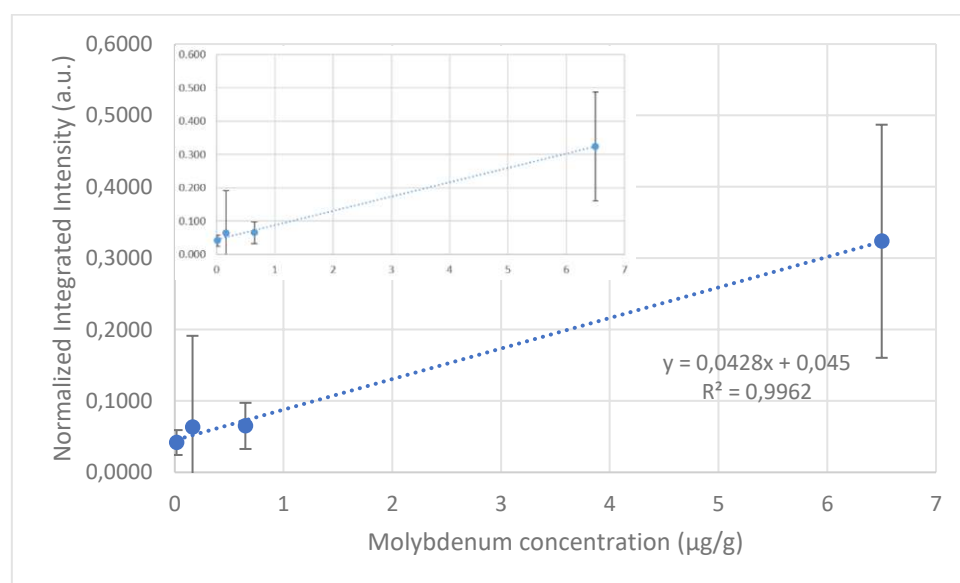


Figure 35 Modified LA-ICP-MS Molybdenum calibration; spray Nafion®; Europium corrected; <sup>13</sup>C normalized; imageGEO193 laser system;(Table 26)

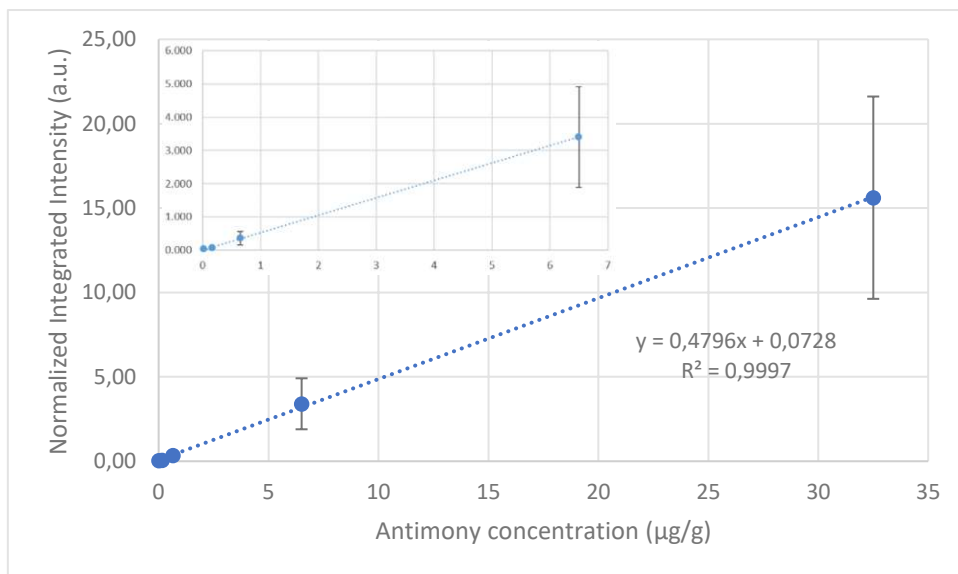


Figure 36 Modified LA-ICP-MS Antimony calibration; spray Nafion®; Europium corrected; <sup>13</sup>C normalized; imageGEO193 laser system;(Table 27)

Table 11 Lead, Zinc, Molybdenum, Zircon, and Antimony LOD and LOQ for Nafion®.

Element	LOD (µg/g)	LOQ (µg/g)
Lead	0.861	4.30
Zinc	1.95	9.77
Molybdenum	0.939	4.69
Zircon	0.724	3.62
Antimony	0.163	0.814

The obtained results needed to be further validated with liquid ICP-MS measurements. This, however, failed due to the disadvantageous properties of Nafion® when high pressure and temperatures are applied to it in a Teflon vessel. It was not possible to dissolve the polymer film in its entirety and fragments of it got stuck to the wall of the container. The removal of the remains turned out to be exceptionally difficult with multiple cleaning extraction being required to gradually remove the contaminants. It was also necessary to mechanically clean the inside of the vessels after every extraction. Further extraction experiments with other extraction solutions were not executed due to fear of destroying the vessels in the process.

## 4.7 Non-Polymer Substrates

Other non-polymer samples were also investigated, given the exceptionally good results on polymers. Aluminum, Copper, glass, low temperature cofired ceramics (= LTCC), silicon wafers, and silicon carbide were chosen as alternate substrates given their availability and widespread use in a multitude of technological applications. The spray process and parameters were kept the same as for the polymer substrates. The prepared samples were further analyzed with LA-ICP-MS line (Figure 12) measurements using the imageGEO193 laser system due to its increased precision and sensitivity. The investigated Isotopes for the calibrations are  $^{66}\text{Zn}$ ,  $^{107}\text{Ag}$ ,  $^{113}\text{In}$ , and  $^{208}\text{Pb}$ . Line scans were chosen to test the calibration quality over a larger surface area. Indium was chosen due to its wide use as an internal standard. Zn, Ag as well as Pb are often found as contaminants in the chosen samples or make up a majority of the substance composition in the case of glass and LTCC.

The samples after the ablation process can be seen in Figure 37. All substrates show an even distribution of residues across the surface area with glass closely resembling those on a polymer substrate. All ablated lines are visible and show even ablation of the material across the whole line and substance.

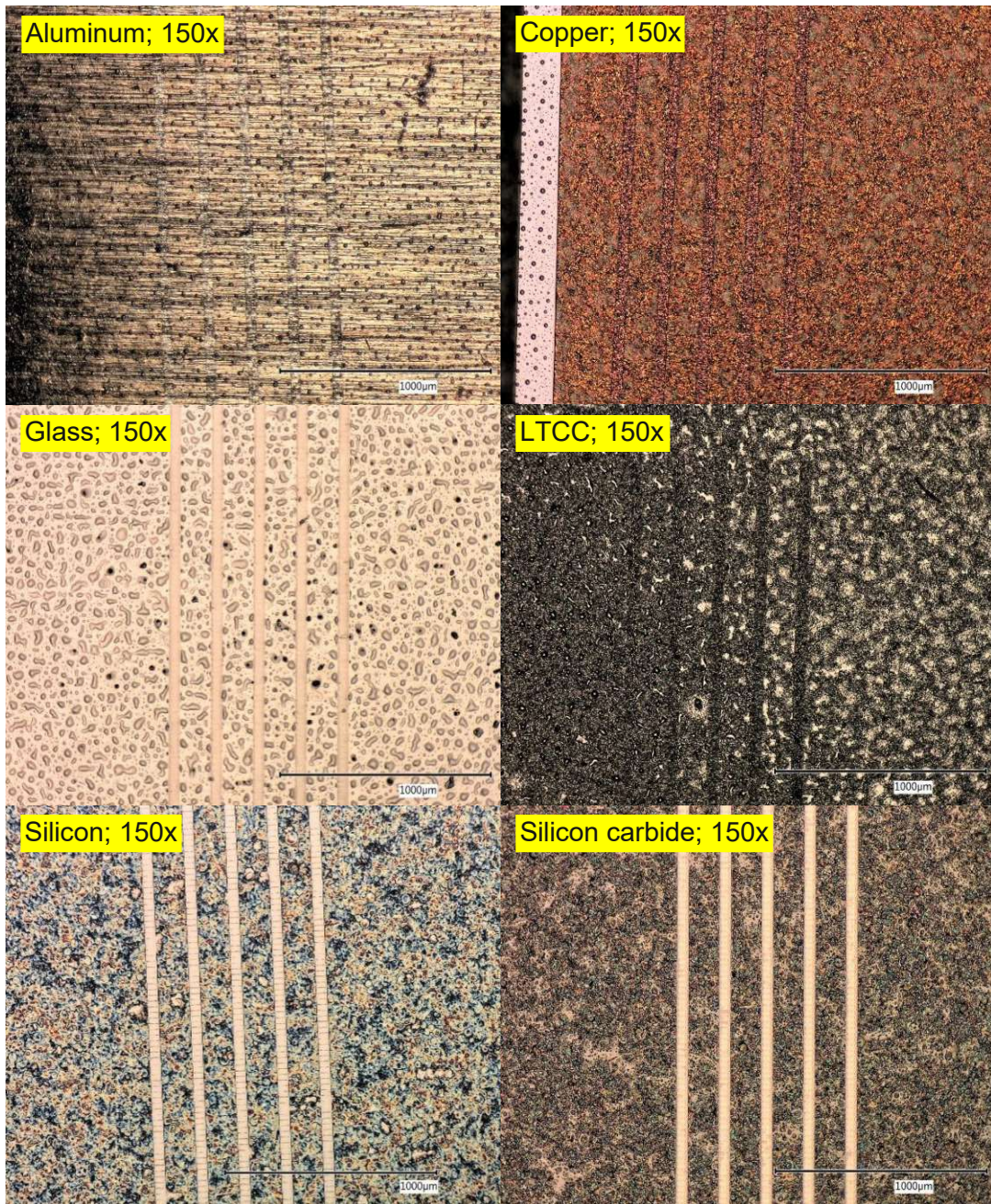


Figure 37 residues and ablation line at 150x of Aluminum (top, left), Copper (top, right), glass (middle, left), LTC (middle, right), silicon (bottom, left), and silicon carbide (bottom, right).

The resulting calibrations with Aluminum as a substrate (Figure 38) show good results for all analytes in the range of 0.05 to 10 µg/g. All elements show linear correlation, nearly no standard deviation, except for Ag, which rules out an inhomogeneous distribution of the analytes in the sample material. Pb shows a significant increase of its intercept, hinting at low contents of Pb being present in Aluminum. Indium (Figure 38 to Figure 43) offers exceptionally good calibrations on all materials, with Aluminum (Figure 38) performing best.

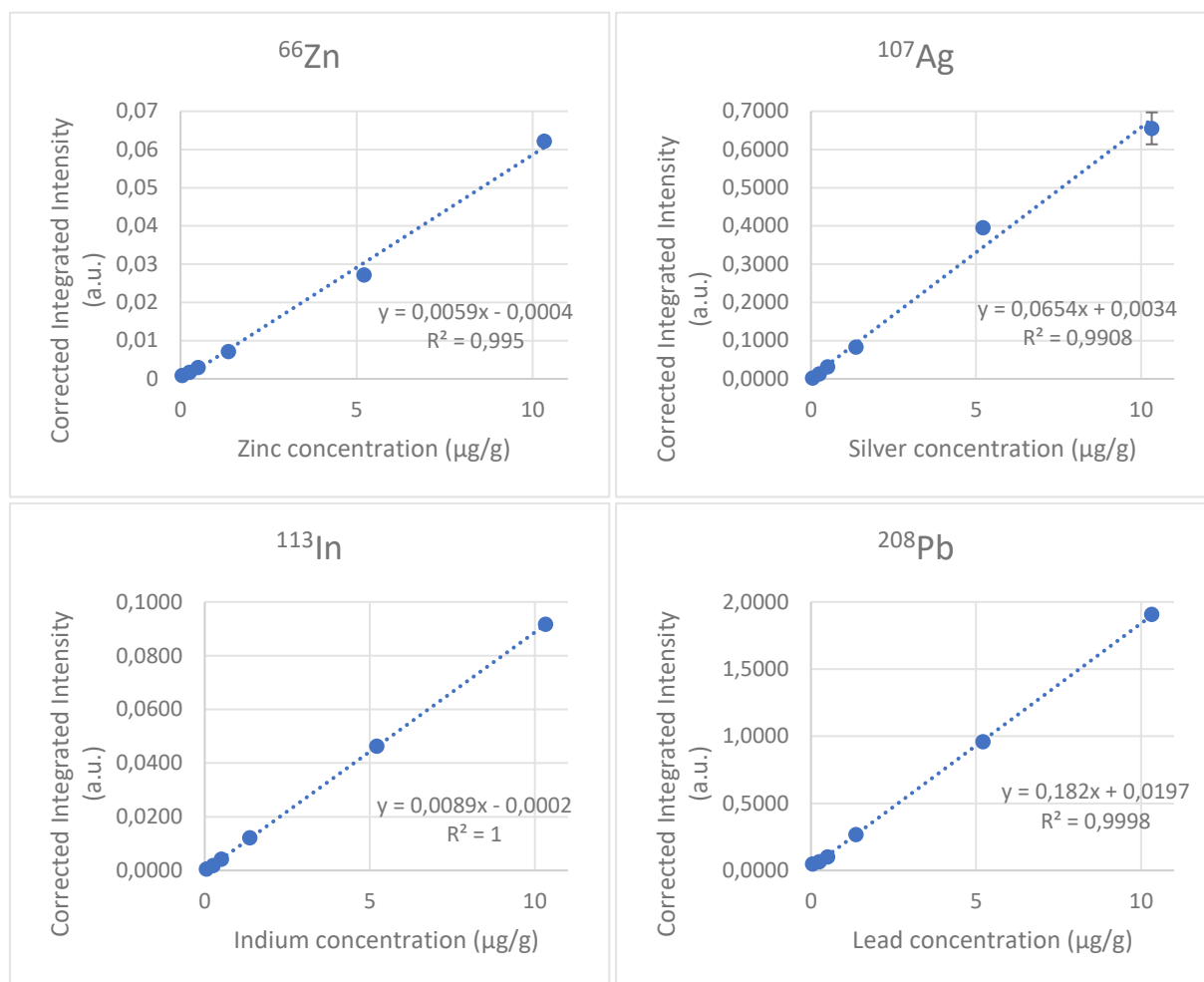


Figure 38 LA-ICP-MS Zinc (top left), Silver (top right), Indium (bottom left), and Lead (bottom right) calibration; spray on Aluminum; Eu corrected; imageGEO193 laser system; (Table 28)

The resulting calibrations with Copper as a substrate (Figure 39) show good results for all analytes in the range of 0.05 to 10 µg/g. All elements show linear correlation, nearly no standard deviation which rules out an inhomogeneous distribution of the analytes in the sample material.  $^{107}\text{Ag}$  shows a significant increase of its intercept, hinting at low contents of Ag being present in Copper, which is very likely.

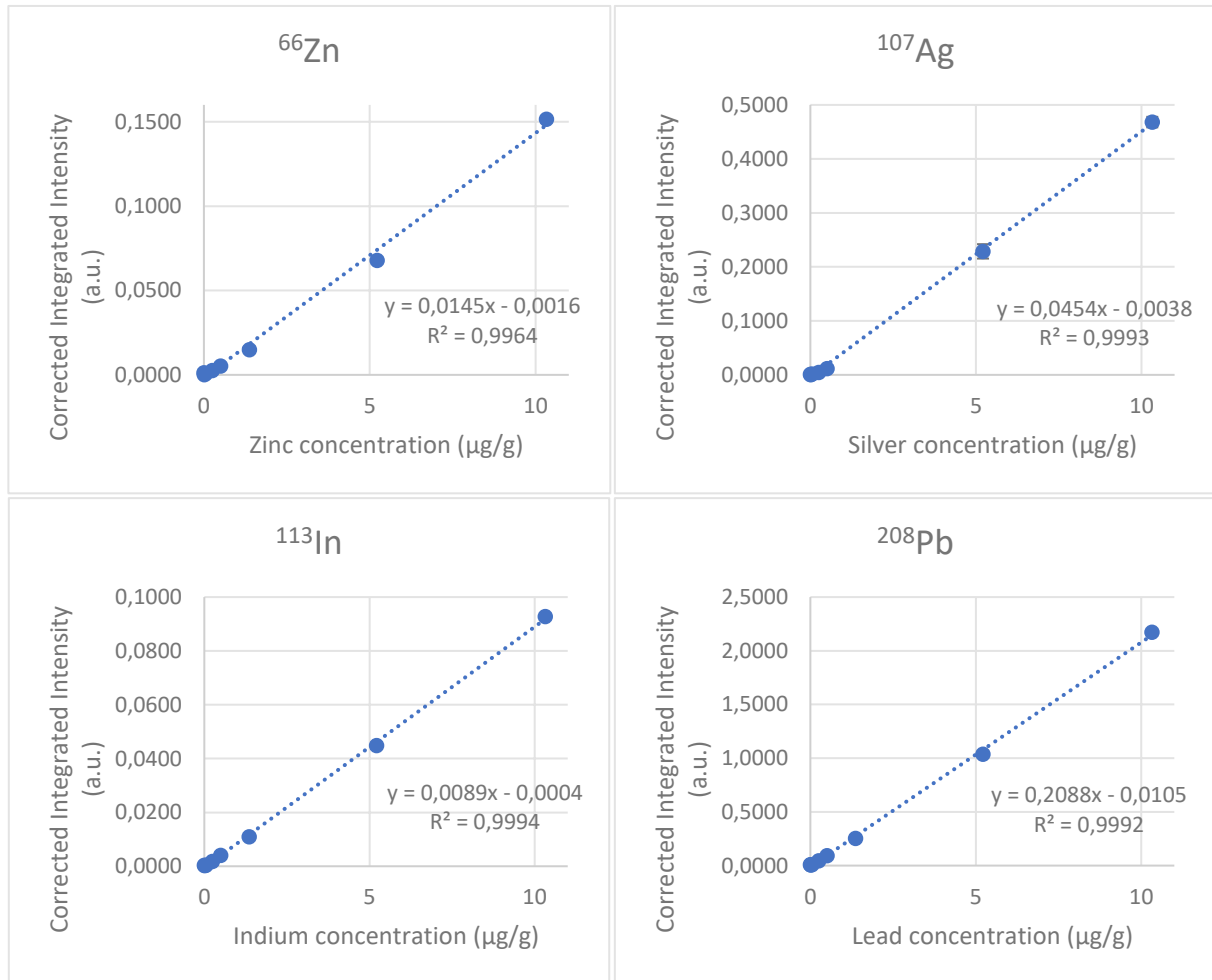


Figure 39 LA-ICP-MS Zinc (top left), Silver (top right), Indium (bottom left), and Lead (bottom right) calibration; spray on Copper; Eu corrected; imageGEO193 laser system; (Table 29)



The resulting calibrations with glass as a substrate (Figure 40) show good results for all analytes in the range of 0.05 to 10 µg/. All elements show linear correlation and nearly no standard deviation which rules out an inhomogeneous distribution of the analytes in the sample material. The measured signals for <sup>66</sup>Zn in the 0.05 to 0.5 µg/g range shows significant deviation from the expected values and was found to contain two outliers. A possible cause for this can be the addition of Zinc oxid (ZnO) in the glass but the low standard deviation as well as the found outliers makes human error during the preparation process a possibility.

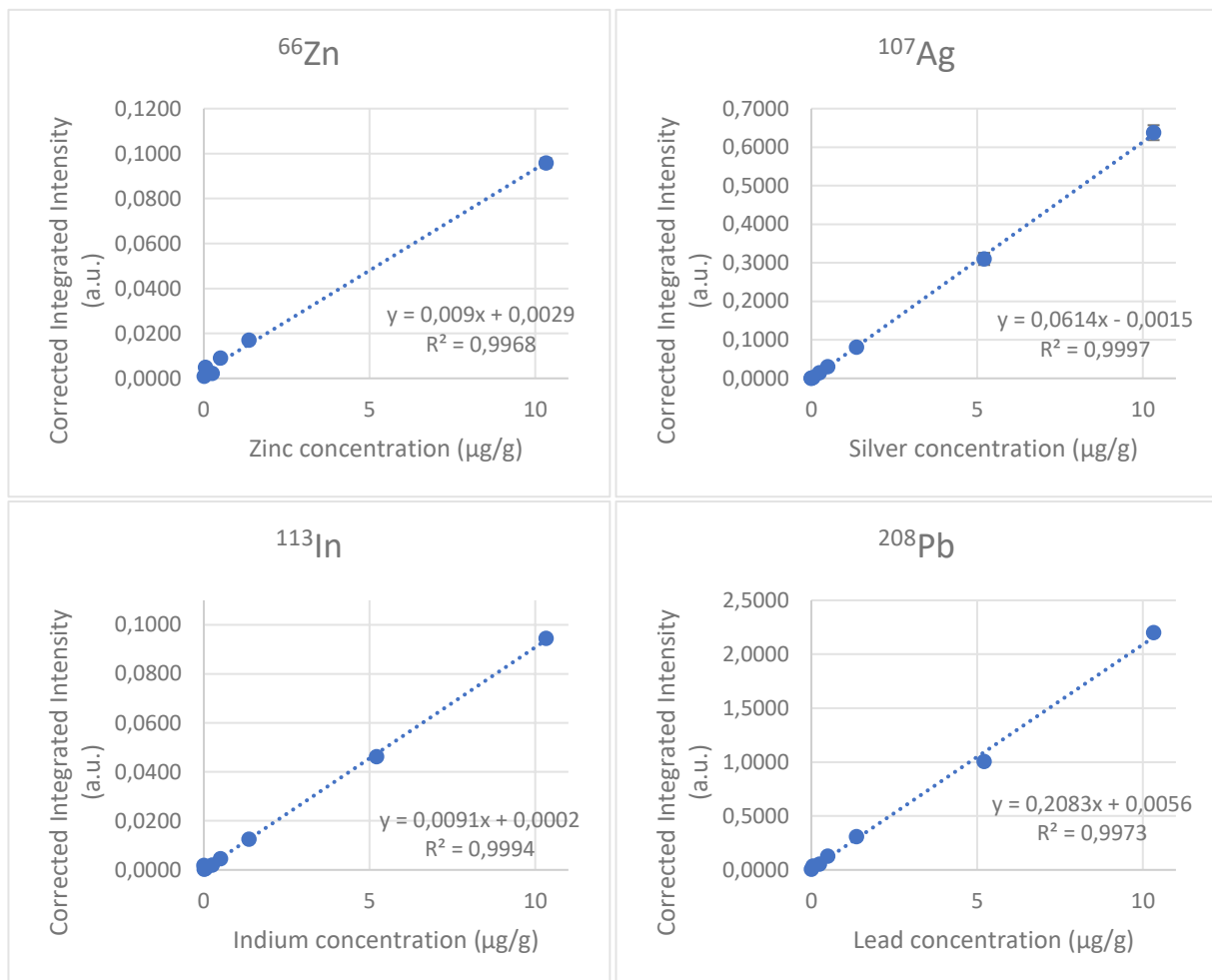


Figure 40 LA-ICP-MS Zinc (top left), Silver (top right), Indium (bottom left), and Lead (bottom right) calibration; spray on glass; Eu corrected; imageGEO193 laser system; (Table 30)

The resulting calibrations with LTCC as a substrate (Figure 41) show good results for Ag and In, decent ones for Zn, and bad ones for Pb in the range of 0.05 to 10 µg/g. It is of note that the investigated sample does contain a high amount of Pb, Al, O, and Zn in the sample material. Ag and In show overall worse calibrations on LTCC but are still considered usable with a good linear correlation and low standard deviation indicating a homogenous distribution of the analytes throughout the sample. Ag also shows a slight increased intercept which hints at low concentrations being present in the investigated sample. Both Zn and Pb have very high backgrounds and intercepts which would demand a calibration in a higher ppm range. Zn is however clearly showing a high intercept value with low standard deviations, which indicates the presence of a homogeneously distributed Zn concentration. Pb especially highlights the need to test a wide range of standard concentrations for unknown substances before a precise sample concentration evaluation can be performed.

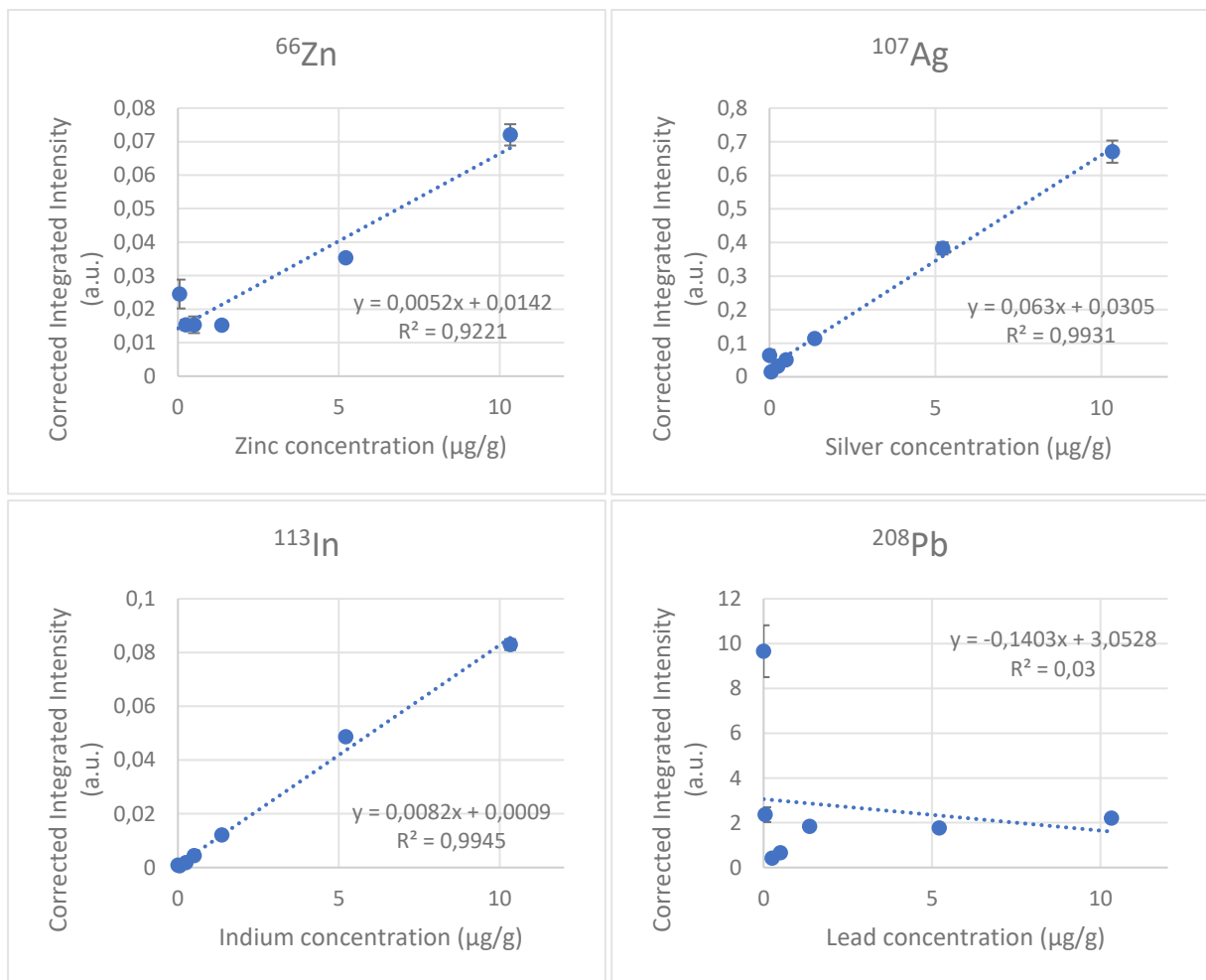


Figure 41 LA-ICP-MS Zinc (top left), Silver (top right), Indium (bottom left), and Lead (bottom right) calibration; spray on LTCC; Eu corrected; imageGEO193 laser system; (Table 31)

The resulting calibrations with silicon as a substrate (Figure 42) show exceptionally good results for all analytes in the range of 0.05 to 10 µg/g with Ag performing slightly worse. All elements show linear correlation and nearly no standard deviation which rules out an inhomogeneous distribution of the analytes in the sample material. A possible cause for Ag performing worse can be human error during the spray process, sample preparation, or the LA-ICP-MS measurement.

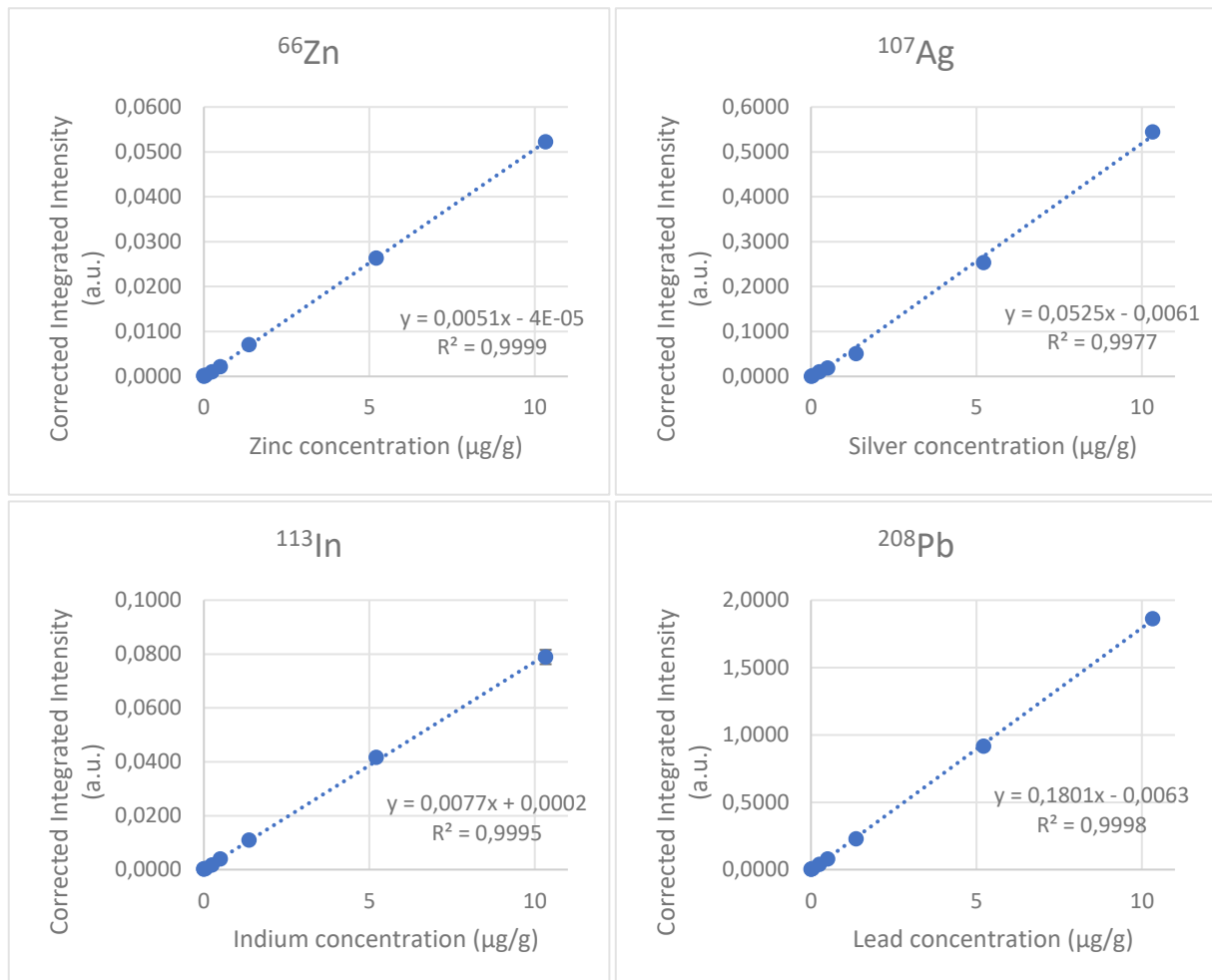


Figure 42 LA-ICP-MS Zinc (top left), Silver (top right), Indium (bottom left), and Lead (bottom right) calibration; spray on silicon; Eu corrected; imageGEO193 laser system; (Table 32)

The resulting calibrations with silicon carbide as a substrate (Figure 43) show exceptionally good results for all analytes in the range of 0.05 to 10 µg/g with Pb performing best. All elements show linear correlation and nearly no standard deviation which rules out an inhomogeneous distribution of the analytes in the sample material. A slight deviation for 5 µg/g In hints at an error during the spray process or during the LA-ICP-MS measurement for this specific sample since there was only one spray solution used for all samples during the simultaneous sample preparation.

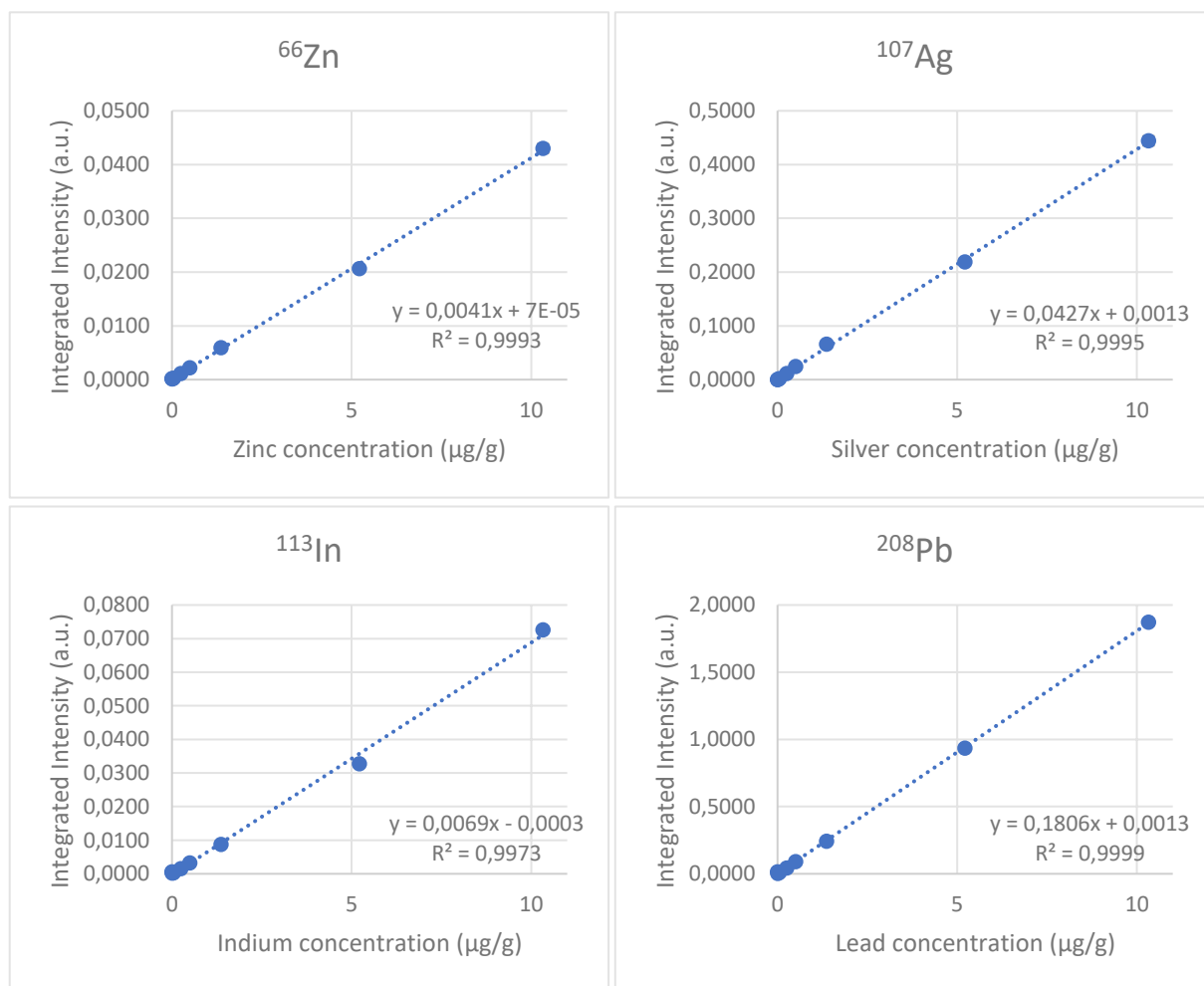


Figure 43 LA-ICP-MS Zinc (top left), Silver (top right), Indium (bottom left), and Lead (bottom right) calibration; spray on silicon carbide; Eu corrected; imageGEO193 laser system; (Table 33)

The performed experiments indicated the presence of the investigated analytes for some substrate materials. However, it was not possible to determine the analyte concentrations in the samples due to the lack of means to determine the removed substrate amount. Quantitative measurements can only be conducted with information about the ablated mass. One possibility would have been a gravimetric approach with weighing the substrate before and after the spray process as well as after the ablation process. An overview of the results can be seen in Table 12.

Table 12 Result overview

Material	Possible contaminants	Sensitivity				Homogenous			
		66Zn	107Ag	113In	203Pb	66Zn	107Ag	113In	203Pb
Aluminum	Pb, Ag	great	great	great	great	Yes	No	Yes	Yes
Copper	Ag	great	great	great	great	Yes	Yes	Yes	Yes
Glass	Zn	good	great	great	good	Yes	No	Yes	Yes
LTCC	Zn, Pb, Ag	decent	good	good	bad	No	Yes	Yes	No
Silicon	x	great	great	great	great	Yes	Yes	Yes	Yes
Silicon Carbide	x	great	great	great	great	Yes	Yes	Yes	Yes

## 5. Conclusion

LA-ICP-MS offers a great way to directly measure solid materials without the need for laborious, time-consuming, and destructive digestion. However, to perform quantitative analysis matrix matched standards are needed, which are often not available in the form of certified reference materials. This work tackled the problem of developing a new method to circumvent the need for those materials by applying the standard directly to the sample, while simultaneously forgoing the disadvantages of the dried droplet method.

The newly developed standard addition method shows promising results as a calibration approach for use in LA-ICP-MS. It offers a great alternative to the dried droplet technique with a more streamlined and automated spray process through the usage of an HTX-Sprayer. The homogenous distribution of the standard on the sample surface allows for large amounts of individual measurements for more detailed information about the investigated sample. This completely removes the “Hot Spot” problem as well as the coffee ring effect from the pool of potential problems, allowing an uncomplicated work process of preparing standards and applying them to the surface without much trouble.

Three polymer films, namely Kapton<sup>®</sup>, Nafion<sup>®</sup>, and polystyrene, were tested as substrate for the calibration method and were found to be suitable for the method. The liquid ICP-MS measurements were used as a reference method to confirm the obtained LA-ICP-MS results due to a lack of a CRM and known concentration provided by the producer. However, only Kapton<sup>®</sup> was found to be a suitable film for the liquid ICP-MS reference method due to low analyte concentrations in polystyrene and critical issues during the digestion process for Nafion<sup>®</sup>. The evaluated Sulfur LA-ICP-MS ( $36.4 \pm 3.12 \mu\text{g/g}$ ) and liquid ICP-MS ( $31.6 \pm 1.98 \mu\text{g/g}$ ) measurements for Kapton<sup>®</sup> are in good accordance, which makes the method fit for purpose to investigate other elements in the same film, such as Zn and Pb, as well as other polymer films despite the lack of a suitable reference.

The developed method is also applicable to thin films with an unknown composition as long as the density and thickness of the material is known or can be researched through experimental means as shown with the Kapton<sup>®</sup> reference measurements for S.

The Zn and Pb calibrations on Kapton<sup>®</sup> were successful but did not yield conclusive results about their concentration in the film since both were found to be below the calculated LOQ and LOD. This can be due to the lack of the investigated analytes in the sample, exceptionally low concentrations, or an inhomogeneous distribution in the film. The liquid ICP-MS reference measurements were found to be yielding 3-times the amount for Pb and 20-times the amount for Zn. Blank spot LA-ICP-MS measurements (n=360) were conducted to investigate the distribution of the elements in the sample. Most measurement locations showed signals in the order of the background, with “hot spots” being

observed showing exceptionally high intensity. The results confirm the assumption of an inhomogeneous distribution, which also explains the extremely high standard deviation (RS = 200 %) in Pb in Kapton®. The higher number of blank measurements also shifted the concentration result towards the liquid ICP-MS reference concentration which is plausible given the large amount of polymer film used for the digestion.

Calibration of Zn and Pb were also created for Polystyrene and Zn, Pb, Sb, Zr, as well as Mo were investigated for Nafion®, with all calibrations showing great linear correlation for a large variety of elements. However, the calculated analyte concentrations were always found to be below the calculated LOQ and LOD for the respective element. The standard deviations for each element have also shown a high degree of inhomogeneous distribution of the target analytes in the samples. There is also no way to confirm the results due to the inability to perform reference liquid ICP-MS measurements because of low concentrations in Polystyrene and digestion issues in Nafion®.

Other non-polymer samples were also investigated. Aluminum, Copper, glass, low temperature cofired ceramics (= LTCC), silicon wafers, and silicon carbide were chosen as alternate substrates given their availability and widespread use in a multitude of technological applications. The sprayed substrates show an even distribution of residues across the surface area with all yielding great linear calibrations in the range of 0.05 to 10 µg/g. Multiple analytes have also been found to be likely contaminants in the measured samples, such as Zn in glass as well as LTCC, Ag in Copper, and Pb in Aluminum. The sensitivity was found to be great for all investigated samples, except for glass and LTCC, which might influence the ablation process due to their amorphous properties. The standard deviation for each measured analyte highlights the ability of this method to investigate the question of inhomogeneity across a wide range of different materials.

Conclusively, the newly developed standard addition method offers exceptionally great linear calibrations for a large concentration range on multiple substrate materials with a large selection of possible analytes.

## 6. Literature / References

- [1] Russo, R.E., Mao, X.L., Liu, H.C., Yoo, J.H., & Mao, S.S. (1999). Time-resolved plasma diagnostics and mass removal during single-pulse laser ablation. *Applied Physics A*, 69, S887-S894. DOI: <https://doi.org/10.1007/s003390051553>
- [2] Limbeck, A., Galler, P., Bonta, M., Bauer, G., Nischkauer, W., & Vanhaecke, F. (2015). Recent advances in quantitative LA-ICP-MS analysis: challenges and solutions in the life sciences and environmental chemistry. *Analytical and bioanalytical chemistry*, 407(22), 6593–6617. DOI: <https://doi.org/10.1007/s00216-015-8858-0>
- [3] YongSheng Liu, Y. Liu, ZhaoChu Hu, Z. Hu, Ming Li, M. Li, & Shan Gao, S. Gao. (0000). Applications of LA-ICP-MS in the elemental analyses of geological samples. *Chinese science bulletin*, 58, 3863-3878. DOI: 10.1007/s11434-013-5901-4
- [4] Cruz-Alonso, M., Lores-Padín, A., Valencia, E., González-Iglesias, H., Fernández, B., & Pereiro, R. (2019). Quantitative mapping of specific proteins in biological tissues by laser ablation-ICP-MS using exogenous labels: aspects to be considered. *Analytical and bioanalytical chemistry*, 411(3), 549–558. DOI: 10.1007/s00216-018-1411-1
- [5] Stehrer, T., Heitz, J., Pedarnig, J.D., Huber, N., Aeschlimann, B., Günther, D., Scherndl, H., Linsmeyer, T., Wolfmeir, H., & Arenholz, E. (2010). LA-ICP-MS analysis of waste polymer materials. *Analytical and Bioanalytical Chemistry*, 398, 415-424. DOI: <https://doi.org/10.1007/s00216-010-3963-6>
- [6] Lin, J. , Liu, Y. , Yang, Y. , & Hu, Z. (2016). Calibration and correction of LA-ICP-MS and LA-MC-ICP-MS analyses for element contents and isotopic ratios. *Solid Earth Sciences*, 1 (1), 5-27. DOI: 10.1016/j.sesci.2016.04.002
- [7] Sylvester, Paul. (2008). CHAPTER 5: MATRIX EFFECTS IN LASER ABLATION-ICP-MS. Mineralogic Association of Canada Short Course. 40.
- [8] DuPont. (2023). Kapton® 100EN. Dupont. <https://www.dupont.com/products/Kapton-100en.html>, accessed on the 13th February 2023.
- [9] Thermo Fisher Scientific Inc. (2023). Fishersci. <https://www.fishersci.at/shop/products/Nafion-r-n-115-membrane-0-125mm-thick-0-90-meq-g-exchange-capacity-thermo-scientific/11369827>, accessed on the 13th February 2023.
- [10] Pasilis, S., P., Ven Berkel, G., J. (2010) Modern Atmospheric Pressure Surface Sampling/Ionization Techniques in Mass Spectrometry. *Encyclopedia of Spectroscopy and Spectrometry* (Second Edition), Academic Press. DOI: 10.1016/B978-0-12-803224-4.00063-7



- [11] Brima, E., I., Jenkins, R., O., Haris, P., I. (2006). Understanding arsenic metabolism through spectroscopic determination of arsenic in human urine. *Spectroscopy*, 20, 125-151. DOI: <https://doi.org/10.1155/2006/759046>
- [12] Bulska, E., & Wagner, B. (2016). Quantitative aspects of inductively coupled plasma mass spectrometry. *Philosophical transactions. Series A, Mathematical, physical, and engineering sciences*, 374(2079), 20150369. DOI: <https://doi.org/10.1098/rsta.2015.0369>
- [13] Halicz, Ludwik. (2004). Quantitative Analysis of Silicates Using LA-ICP-MS with Liquid Calibration. *Journal of Analytical Atomic Spectrometry*, 19(12), 1539-1545. DOI: 10.1039/b410132d
- [14] Fernández, B., Claverie, F., Pécheyran, C., & Donard, O.F. (2007). Direct analysis of solid samples by fs-LA-ICP-MS. *Trends in Analytical Chemistry*, 26, 951-966. DOI: <https://doi.org/10.1016/j.trac.2007.08.008>.
- [15] Fricker, Mattias & Günther, Detlef. (2016). Instrumentation, Fundamentals, and Application of Laser Ablation-Inductively Coupled Plasma-Mass Spectrometry. DOI: 10.1007/978-3-662-49894-1\_1
- [16] Svelto O. (1976) Principles of Lasers, Springer Science+Business Media, LLC, DOI: 10.1007/978-1-4899-2748-4
- [17] Koechner, W. (2006). Solid-State Laser Engineering, Springer New York, NY, DOI: <https://doi.org/10.1007/0-387-29338-8>
- [18] Dinesh, P., Balasubramanian, K., R., Buvanashakaran, G., Naidu., (2011). Laser surface hardening: A review. *International Journal of Surface Science and Engineering*, 5, (2/3) 131 - 151. DOI: 10.1504/IJSURFSE.2011.041398
- [19] Uemoto, M. (2011) Instrumental Chemical Analysis of Magnesium and Magnesium Alloys. Magnesium Alloys - Corrosion and Surface Treatments, DOI: 10.5772/13727
- [20] Montaser, A. (1998) Inductively Coupled Plasma Mass spectrometry, Wiley-VCH.
- [21] Tantra, R. (2016) Nanomaterial Characterization An Introduction, Wiley. DOI: 10.1002/9781118753460
- [22] Gross, J., G. (2011) Mass Spectrometry (2), Springer. DOI: <https://doi.org/10.1007/978-3-319-54398-7>
- [23] Honour J. W. (2003). Benchtop mass spectrometry in clinical biochemistry. *Annals of clinical biochemistry*, 40(Pt 6), 628–638. DOI: <https://doi.org/10.1258/000456303770367216>

- [24] HTXImaging (2020). HTX TM-Sprayer™. Htximaging. <http://www.htximaging.com/tm-sprayer>, accessed on the 19th April 2023.
- [25] Miliszkiwicz, N., Walas, S., & Tobiasz, A. (2015). Current approaches to calibration of LA-ICP-MS analysis. *Journal of Analytical Atomic Spectrometry*, *30*, 327-338. DOI: 10.1039/C4JA00325J
- [26] Zhang, S., He, M., Yin, Z., Zhu, E., Hang, W., & Huang, B. (2016). Elemental fractionation and matrix effects in laser sampling based spectrometry. *Journal of Analytical Atomic Spectrometry*, *31*, 358-382. DOI: 10.1039/C5JA00273G
- [27] Olivares, I.R., Souza, G.B., Nogueira, A.R., Toledo, G.T., & Marcki, D.C. (2018). Trends in developments of certified reference materials for chemical analysis - Focus on food, water, soil, and sediment matrices. *Trends in Analytical Chemistry*, *100*, 53-64. DOI: 10.1016/j.trac.2017.12.013
- [28] Wise S. A. (2018). What is novel about certified reference materials?. *Analytical and bioanalytical chemistry*, *410(8)*, 2045–2049. DOI: <https://doi.org/10.1007/s00216-018-0916-y>
- [29] International Standards Organization (ISO) (2016) General requirements for competence of reference material producers. ISO Guide 17034. <https://www.iso.org/standard/29357.html>
- [30] Garbe-Schönberg, D., & Müller, S. (2014). Nano-particulate pressed powder tablets for LA-ICP-MS. *Journal of Analytical Atomic Spectrometry*, *29*, 990-1000. DOI: 10.1039/c4ja00007b
- [31] Nischkauer, W., Vanhaecke, F., & Limbeck, A. (2016). Self-aliquoting micro-grooves in combination with laser ablation-ICP-mass spectrometry for the analysis of challenging liquids: quantification of Lead in whole blood. *Analytical and bioanalytical chemistry*, *408(21)*, 5671–5676. DOI: <https://doi.org/10.1007/s00216-016-9717-3>
- [32] Horak, F., Nagl, A., Föttinger, K., & Limbeck, A. (2020). Application of micro-dried droplets for quantitative analysis of particulate inorganic samples with LA-ICP-MS demonstrated on surface-modified nanoparticle TiO<sub>2</sub> catalyst materials. *Mikrochimica acta*, *187(12)*, 641. DOI: <https://doi.org/10.1007/s00604-020-04609-9>
- [33] Pabst, M., Fagerer, S. R., Köhling, R., Küster, S. K., Steinhoff, R., Badertscher, M., Wahl, F., Dittrich, P. S., Jefimovs, K., & Zenobi, R. (2013). Self-aliquoting microarray plates for accurate quantitative matrix-assisted laser desorption/ionization mass spectrometry. *Analytical chemistry*, *85(20)*, 9771–9776. DOI: <https://doi.org/10.1021/ac4021775>
- [34] Foltynová, P., Kanický, V., & Preisler, J. (2012). Diode laser thermal vaporization inductively coupled plasma mass spectrometry. *Analytical chemistry*, *84(5)*, 2268–2274. DOI: <https://doi.org/10.1021/ac202884m>

- [35] Villaseñor, Á., Sánchez, R., Bocconcelli, M., & Todolí, J. L. (2021). Localized Quantitative Analysis of Polymeric Films through Laser Ablation-Inductively Coupled Plasma Mass Spectrometry. *Polymers*, *13*(3), 345. DOI: <https://doi.org/10.3390/polym13030345>
- [36] Yunker, P. J., Still, T., Lohr, M. A., & Yodh, A. G. (2011). Suppression of the coffee-ring effect by shape-dependent capillary interactions. *Nature*, *476*(7360), 308–311. DOI: <https://doi.org/10.1038/nature10344>
- [37] O'Rourke, M. B., Djordjevic, S. P., & Padula, M. P. (2018). The quest for improved reproducibility in MALDI mass spectrometry. *Mass spectrometry reviews*, *37*(2), 217–228. DOI: <https://doi.org/10.1002/mas.21515>
- [38] Thermo Scientific™. (2023). iCAP™ TQ ICP-MS. thermofischer. <https://www.thermofisher.com/order/catalog/product/BRE731436> accessed on 8th of May 2023.
- [39] imageGEO193. (2022) Designed for the next generation of geochemical analysis. icpmslasers. <http://www.icpmslasers.com/laserablation/nwrimageGEO/> accessed on the 25th of May 2022
- [40] kenelec scientific. (2022). ESL NWR213 Laser Ablation System. kenelec. <https://www.kenelec.com.au/products/esi-nwr213-laser-ablation-system/> accessed on the 25th of May 2022.
- [41] Anton Paar (2022) Multiwave 5000. anton-paar. <https://www.anton-paar.com/at-de/produkte/details/multiwave-5000/> accessed on the 25th of May 2022.
- [42] DuPont. (2023). dupont. <https://www.dupont.com/content/dam/dupont/amer/us/en/ei-transformation/public/images/banner/DEC-Kapton-roll-2x1.jpg> asseced on the 8th of May 2023.
- [43] Horak, F., & Limbeck, A. (2016).  $\mu$ -Dried-Droplets as standards for daily performance checks in single particle LIBS/LA-ICP-MS. In *Book of Abstracts* (p. 94). National Institute of Chemistry Slovenia. <http://hdl.handle.net/20.500.12708/49517>
- [44] Bonta, M., Lohninger, H., Laszlo, V., Hegedus, B., Limbeck, A. (2014) Quantitative LA-ICP-MS imaging of platinum in chemotherapy treated human malignant pleural mesothelioma samples using printed patterns as standard. *J. Anal. At. Spectrom*, *29*, 2159-2167. DOI: 10.1039/C4JA00245H

## 7. Appendix

Table 13 Indium standard kalibration; liquid ICP-MS; normalized  $^{115}\text{In}/^{157}\text{Gd}$

Indium concentration (ng/g)	Normalized signal $^{115}\text{In}/^{157}\text{Gd}$ (a.u)
0.1	0.4601
0.5	2.272
2	9.343
10	47.76

Table 14 Data for Area specific mass deposition calculation

Normalized signal sample $^{115}\text{In}/^{157}\text{Gd}$ (a.u)	$c_{cal}$ (ppm)	$m_{ges}$ (g)	$m_{digest}$ (g)	$m_{sample}$ (g)
1.76	0.390	8.93	13.4	2.34
1.71	0.382	8.93	13.2	2.31
1.67	0.372	8.91	13.3	2.31
1.66	0.371	8.92	13.5	2.33
1.72	0.371	8.95	13.5	2.35
1.81	0.391	8.96	13.1	2.37
1.73	0.373	8.96	13.1	2.37
1.89	0.407	9.19	13.3	2.61

Table 15 LA-ICP-MS Sulfur calibration data

Sulfur concentration ( $\mu\text{g/g}$ )	Modified Sulfur concentration ( $\mu\text{g/g}$ )	Eu Corrected and normalized signal sample $^{32}\text{S}/^{13}\text{C}$ (a.u.)	Standard deviation (a.u.)
0	0	0.1096	0.0132
5.25	12.1	0.1452	0.0254
10.3	23.7	0.1518	0.0261
25.4	58.5	0.2853	0.0300
50.7	117	0.3875	0.0630
102	235	0.8212	0.1751
153	351	1.2035	0.1792

Table 16 liquid ICP-MS Sulfur calibration data

Sulfur concentration ( $\mu\text{g/g}$ )	$^{32}\text{S}$ Signal (a.u.)	Normalized signal sample $^{32}\text{S}/^{157}\text{Gd}$ (a.u.)
0	14850	0.3167
12.5	31429	0.7107
25	46813	0.9595
50	78897	1.636
125	174199	3.624
250	327373	6.890
500	621927	13.21
1000	1215942	25.79

Table 17 LA-ICP-MS Lead calibration data

Lead concentration ( $\mu\text{g/g}$ )	Modified Lead concentration ( $\mu\text{g/g}$ )	Eu Corrected and normalized signal sample $^{208}\text{Pb}/^{13}\text{C}$ (a.u.)	Standard deviation (a.u.)
0.001	0.0023	0.0002	0.0001
0.01	0.0231	0.0004	0.0001
0.025	0.0576	0.0008	0.0001
0.05	0.1153	0.0016	0.0002
0.1	0.2306	0.0029	0.0004
0.5	1.153	0.0170	0.0019

Table 18 LA-ICP-MS Zinc calibration data

Zinc concentration ( $\mu\text{g/g}$ )	Modified Zinc concentration ( $\mu\text{g/g}$ )	Eu Corrected and normalized signal sample $^{64}\text{Zn}/^{13}\text{C}$ (a.u.)	Standard deviation (a.u.)
0.01	0.0231	0.0003	0.0001
0.1	0.2306	0.0004	0.0001
0.25	0.5764	0.0007	0.0002
0.5	1.153	0.0012	0.0003
1	2.306	0.0022	0.0003
5	11.53	0.0100	0.0012

Table 19 liquid ICP-MS Zinc calibration data

Zinc concentration ( $\mu\text{g/g}$ )	Normalized signal sample $^{64}\text{Zn}/^{158}\text{Gd}$ (a.u.)
0	0.1226
0.1	0.1435
0.5	0.2796
1	0.4123
5	1.567
10	2.978
25	7.539

Table 20 liquid ICP-MS Lead calibration data

Lead concentration ( $\mu\text{g/g}$ )	Normalized signal sample $^{208}\text{Pb}/^{158}\text{Gd}$ (a.u.)
0	0.1382
0.1	0.4499
0.5	1.626
1	3.202
5	14.64
10	29.05
25	72.33

Table 21 LA-ICP-MS Zinc calibration data Polystyrene

Zinc concentration ( $\mu\text{g/g}$ )	Modified Zinc concentration ( $\mu\text{g/g}$ )	Eu Corrected and normalized signal sample $^{64}\text{Zn}/^{13}\text{C}$ (a.u.)	Standard deviation (a.u.)
0.025	0.050	0.0005	0.0014
0.25	0.498	0.0012	0.0005
1	1.99	0.0008	0.0002
10	19.9	0.0065	0.0014
50	99.5	0.0339	0.0083

Table 22 LA-ICP-MS Lead calibration data Polystyrene

Lead concentration ( $\mu\text{g/g}$ )	Modified Lead concentration ( $\mu\text{g/g}$ )	Eu Corrected and normalized signal sample $^{208}\text{Pb}/^{13}\text{C}$ (a.u.)	Standard deviation (a.u.)
0.025	0.0498	0.0002	0.0001
0.25	0.4975	0.0016	0.0006
1	1.99	0.0086	0.0031
10	19.9	0.0873	0.0213
50	99.5	0.5306	0.0942

Table 23 LA-ICP-MS Zinc calibration data Nafion®

Zinc concentration ( $\mu\text{g/g}$ )	Modified Zinc concentration ( $\mu\text{g/g}$ )	Eu Corrected and normalized signal sample $^{64}\text{Zn}/^{13}\text{C}$ (a.u.)	Standard deviation (a.u.)
0.025	0.01625	0.0192	0.0068
0.25	0.1625	0.0162	0.0031
1	0.65	0.0196	0.0042
5	3.25	0.0480	0.0098
50	32.5	0.2593	0.0395

Table 24 LA-ICP-MS Lead calibration data Nafion®; outlier **red**

Lead concentration ( $\mu\text{g/g}$ )	Modified Lead concentration ( $\mu\text{g/g}$ )	Eu Corrected and normalized signal sample $^{208}\text{Pb}/^{13}\text{C}$ (a.u.)	Standard deviation (a.u.)
0.025	0.01625	0.0042	0.0011
0.25	0.1625	0.0120	0.0032
1	0.65	0.0567	0.0073
5	3.25	0.5344	0.0736
<b>50</b>	<b>32.5</b>	<b>4.843</b>	<b>1.040</b>

Table 25 LA-ICP-MS Zircon calibration data Nafion®; outlier red

Zircon concentration (µg/g)	Modified Zircon concentration (µg/g)	Eu Corrected and normalized signal sample <sup>90</sup> Zr/ <sup>13</sup> C (a.u.)	Standard deviation (a.u.)
0.025	0.01625	0.0056	0.0040
0.25	0.1625	0.0322	0.0328
1	0.65	0.1583	0.0859
10	6.5	3.435	1.933
<b>50</b>	<b>32.5</b>	<b>22.37</b>	<b>9.884</b>

Table 26 LA-ICP-MS Molybdenum calibration data Nafion®; outlier red

Molybdenum concentration (µg/g)	Modified Molybdenum concentration (µg/g)	Eu Corrected and normalized signal sample <sup>98</sup> Mo/ <sup>13</sup> C (a.u.)	Standard deviation (a.u.)
50	32.5	3.226	1.374
10	6.5	0.3237	0.1633
1	0.65	0.0651	0.0323
10	6.5	0.3237	0.1633
<b>50</b>	<b>32.5</b>	<b>3.226</b>	<b>1.374</b>

Table 27 LA-ICP-MS Antimony calibration data Nafion®

Antimony concentration (µg/g)	Modified Antimony concentration (µg/g)	Eu Corrected and normalized signal sample <sup>121</sup> Sb/ <sup>13</sup> C (a.u.)	Standard deviation (a.u.)
0.025	0.01625	0.0291	0.0176
0.25	0.1625	0.0645	0.0575
1	0.65	0.3503	0.2067
10	6.5	3.404	1.511
50	32.5	15.62	5.994



Table 28 LA-ICP-MS calibration data Aluminum

Element Concentration (µg/g)	Eu Corrected signal <sup>66</sup> Zn (a.u.)	Eu Corrected signal <sup>107</sup> AG (a.u.)	Eu Corrected signal <sup>113</sup> In (a.u.)	Eu Corrected signal <sup>208</sup> Pb (a.u.)
0	0.0100	0.0004	0.0001	0.1240
0.05	0.0009	0.0019	0.0004	0.0470
0.25	0.0017	0.0125	0.0018	0.0645
0.5	0.0030	0.0312	0.0041	0.1000
1.5	0.0072	0.0830	0.0121	0.2664
5	0.0272	0.3953	0.0462	0.9585
10	0.0622	0.6554	0.0916	1.906
250	0.2394	1.729	0.2310	4.954
Element Concentration (µg/g)	Standard deviation signal <sup>66</sup> Zn (a.u.)	Standard deviation signal <sup>107</sup> AG (a.u.)	Standard deviation signal <sup>113</sup> In (a.u.)	Standard deviation signal <sup>208</sup> Pb (a.u.)
0	0.00070	0.00040	0.00006	0.00780
0.05	0.00001	0.00007	0.00002	0.00060
0.25	0.00007	0.00029	0.00004	0.00177
0.5	0.00007	0.00088	0.00007	0.00231
1.5	0.00015	0.00225	0.00019	0.00344
5	0.00032	0.00929	0.00041	0.00531
10	0.00098	0.04176	0.00104	0.01781
250	0.00887	0.06191	0.00241	0.03706

Table 29 LA-ICP-MS calibration data Copper

Element Concentration (µg/g)	Eu Corrected signal <sup>66</sup> Zn (a.u.)	Eu Corrected signal <sup>107</sup> AG (a.u.)	Eu Corrected signal <sup>113</sup> In (a.u.)	Eu Corrected signal <sup>208</sup> Pb (a.u.)
0	0.0012	0.0013	0.0004	0.0074
0.01	0.0002	0.0003	0.0002	0.0038
0.05	0.0006	0.0014	0.0004	0.0091
0.25	0.0025	0.0048	0.0018	0.0444
0.5	0.0053	0.0120	0.0040	0.0928
1.5	0.0149	0.0307	0.0109	0.2525

5	0.0679	0.2287	0.0448	1.0360
10	0.1516	0.4681	0.0927	2.170
250	0.3748	1.302	0.2211	5.428
Element Concentration (µg/g)	Standard deviation signal <sup>66</sup> Zn (a.u.)	Standard deviation signal <sup>107</sup> AG (a.u.)	Standard deviation signal <sup>113</sup> In (a.u.)	Standard deviation signal <sup>208</sup> Pb (a.u.)
0	0.00081	0.00017	0.00002	0.00020
0.01	0.00001	0.00003	0.00001	0.00005
0.05	0.00002	0.00010	0.00003	0.00011
0.25	0.00007	0.00048	0.00002	0.00081
0.5	0.00010	0.00077	0.00017	0.00066
1.5	0.00023	0.00117	0.00036	0.00426
5	0.00072	0.01334	0.00106	0.01299
10	0.00103	0.00974	0.00072	0.02954
250	0.00177	0.05368	0.00116	0.00624

Table 30 LA-ICP-MS calibration data glass; outlier red

Element Concentration (µg/g)	Eu Corrected signal <sup>66</sup> Zn (a.u.)	Eu Corrected signal <sup>107</sup> AG (a.u.)	Eu Corrected signal <sup>113</sup> In (a.u.)	Eu Corrected signal <sup>208</sup> Pb (a.u.)
0	0.0563	0.0005	0.0018	0.2515
0.01	0.0010	0.0003	0.0002	0.0064
0.05	0.0050	0.0024	0.0005	0.0356
0.25	0.0022	0.0149	0.0020	0.0516
0.5	0.0090	0.0302	0.0045	0.1256
1.5	0.0170	0.0811	0.0125	0.3091
5	0.0189	0.3100	0.0462	1.004
10	0.0958	0.6377	0.0944	2.198
250	0.2351	1.612	0.2378	5.490
Element Concentration (µg/g)	Standard deviation signal <sup>66</sup> Zn (a.u.)	Standard deviation signal <sup>107</sup> AG (a.u.)	Standard deviation signal <sup>113</sup> In (a.u.)	Standard deviation signal <sup>208</sup> Pb (a.u.)
0	0.00279	0.00022	0.00023	0.01878
0.01	0.00004	0.00001	0.00001	0.00029

0.05	0.00006	0.00005	0.00003	0.00194
0.25	0.00004	0.00010	0.00002	0.00107
0.5	0.00021	0.00046	0.00017	0.00268
1.5	0.00016	0.00126	0.00014	0.00261
5	0.00024	0.01577	0.00028	0.00831
10	0.00219	0.01936	0.00116	0.01248
250	0.00158	0.01793	0.00107	0.04038

Table 31 LA-ICP-MS calibration data LTCC; outlier *red*

Element Concentration (µg/g)	Eu Corrected signal <sup>66</sup> Zn (a.u.)	Eu Corrected signal <sup>107</sup> AG (a.u.)	Eu Corrected signal <sup>113</sup> In (a.u.)	Eu Corrected signal <sup>208</sup> Pb (a.u.)
0	<b>0.1948</b>	0.0645	0.0008	9.659
0.05	0.0245	0.0147	0.0006	2.360
0.25	0.0153	0.0322	0.0018	0.4144
0.5	0.0153	0.0504	0.0044	0.6524
1.5	0.0153	0.1143	0.0121	1.836
5	0.0353	0.3825	0.0487	1.762
10	0.0720	0.6704	0.0830	2.201
Element Concentration (µg/g)	Standard deviation signal <sup>66</sup> Zn (a.u.)	Standard deviation signal <sup>107</sup> AG (a.u.)	Standard deviation signal <sup>113</sup> In (a.u.)	Standard deviation signal <sup>208</sup> Pb (a.u.)
0	0.02262	0.01572	0.00008	1.1581
0.05	0.00431	0.00158	0.00004	0.33032
0.25	0.00154	0.00222	0.00003	0.01388
0.5	0.00248	0.00194	0.00006	0.09423
1.5	0.00031	0.00339	0.00030	0.06627
5	0.00056	0.01835	0.00054	0.09206
10	0.00318	0.03302	0.00201	0.03870

Table 32 LA-ICP-MS calibration data silicon

Element Concentration (µg/g)	Eu Corrected signal <sup>66</sup> Zn (a.u.)	Eu Corrected signal <sup>107</sup> AG (a.u.)	Eu Corrected signal <sup>113</sup> In (a.u.)	Eu Corrected signal <sup>208</sup> Pb (a.u.)
0	0.0002	0.0000	0.0003	0.0042
0.01	0.0001	0.0002	0.0002	0.0034
0.05	0.0003	0.0019	0.0003	0.0080
0.25	0.0010	0.0105	0.0017	0.0383
0.5	0.0022	0.0188	0.0039	0.0786
1.5	0.0071	0.0512	0.0110	0.2287
5	0.0263	0.2534	0.0417	0.9151
10	0.0522	0.5449	0.0789	1.864
250	0.1450	1.468	0.2043	4.925
Element Concentration (µg/g)	Standard deviation signal <sup>66</sup> Zn (a.u.)	Standard deviation signal <sup>107</sup> AG (a.u.)	Standard deviation signal <sup>113</sup> In (a.u.)	Standard deviation signal <sup>208</sup> Pb (a.u.)
0	0.00015	0.00004	0.00004	0.00018
0.01	0.00001	0.00001	0.00002	0.00007
0.05	0.00003	0.00001	0.00003	0.00014
0.25	0.00003	0.00013	0.00004	0.00043
0.5	0.00004	0.00053	0.00006	0.00128
1.5	0.00014	0.00081	0.00007	0.00245
5	0.00020	0.00304	0.00111	0.00538
10	0.00043	0.00414	0.00266	0.01146
250	0.00314	0.06201	0.00274	0.04955

Table 33 LA-ICP-MS calibration data silicon carbide

Element Concentration (µg/g)	Eu Corrected signal <sup>66</sup> Zn (a.u.)	Eu Corrected signal <sup>107</sup> AG (a.u.)	Eu Corrected signal <sup>113</sup> In (a.u.)	Eu Corrected signal <sup>208</sup> Pb (a.u.)
0	0.0002	0.0001	0.0006	0.0143
0.01	0.0001	0.0002	0.0002	0.0038
0.05	0.0002	0.0020	0.0003	0.0089
0.25	0.0011	0.0117	0.0015	0.0436

0.5	0.0022	0.0242	0.0033	0.0904
1.5	0.0059	0.0661	0.0088	0.2433
5	0.0206	0.2188	0.0328	0.9355
10	0.0430	0.4441	0.0726	1.871
250	0.1277	1.282	0.1969	4.815
Element Concentration (µg/g)	Standard deviation signal <sup>66</sup> Zn (a.u.)	Standard deviation signal <sup>107</sup> Ag (a.u.)	Standard deviation signal <sup>113</sup> In (a.u.)	Standard deviation signal <sup>208</sup> Pb (a.u.)
0	0.00012	0.00013	0.00013	0.00043
0.01	0.00018	0.00002	0.00001	0.00013
0.05	0.00005	0.00004	0.00001	0.00006
0.25	0.00002	0.00025	0.00003	0.00032
0.5	0.00004	0.00090	0.00005	0.00050
1.5	0.00022	0.00184	0.00015	0.00188
5	0.00014	0.00437	0.00013	0.00427
10	0.00085	0.00877	0.00078	0.00984
250	0.00136	0.03065	0.00141	0.01824